Received: 14 March 2019 | Revised: 8 June 2019 | Accepted: 7 July 2019

DOI: 10.1111/tbed.13293

ORIGINAL ARTICLE

Transboundary and Emerging Diseases WILEY

Positive selection pressure on E2 protein of classical swine fever virus drives variations in virulence, pathogenesis and antigenicity: Implication for epidemiological surveillance in endemic areas

Liani Coronado[1] | Liliam Rios[2] | María Teresa Frías[1] | Laymara Amarán[3] | Paula Naranjo[4] | María Irian Percedo[1] | Carmen Laura Perera[1] | Felix Prieto[3] | Osvaldo Fonseca-Rodriguez[5] | Lester J. Perez[6,7]

[1]Centro Nacional de Sanidad Agropecuaria (CENSA), OIE Collaborating Centre for Diagnosis and Risk Analysis of the Caribbean Region, La Habana, Cuba

[2]Reiman Cancer Research Laboratory, Faculty of Medicine, University of New Brunswick, Saint John, New Brunswick, Canada

[3]National Laboratory for Veterinary Diagnostic (NLVD), La Habana, Cuba

[4]Veterinary Medicine Institute, Havana, Cuba

[5]Department of Epidemiology and Global Health, Umeå University, Umeå, Sweden

[6]Department of Clinical Veterinary Medicine, College of Veterinary Science, University of Illinois, Urbana, IL, USA

[7]College of Veterinary Science, Veterinary Diagnostic Laboratory (VDL), University of Illinois, Urbana, IL, USA

Correspondence
Lester J. Perez, Department of Clinical Veterinary Medicine, College of Veterinary Science, University of Illinois, Urbana, IL, 61802, USA.
Email: ljperez@illinois.edu

Funding information
Program of exotic diseases of Cuba

Abstract

Classical swine fever (CSF), caused by CSF virus (CSFV), is considered one of the most important infectious diseases with devasting consequences for the pig industry. Recent reports describe the emergence of new CSFV strains resulting from the action of positive selection pressure, due mainly to the bottleneck effect generated by ineffective vaccination. Even though a decrease in the genetic diversity of the positively selected CSFV strains has been observed by several research groups, there is little information about the effect of this selective force on the virulence degree, antigenicity and pathogenicity of this type of strains. Hence, the aim of the current study was to determine the effect of the positive selection pressure on these three parameters of CSFV strains, emerged as result of the bottleneck effects induced by improper vaccination in a CSF-endemic area. Moreover, the effect of the positively selected strains on the epidemiological surveillance system was assessed. By the combination of in vitro, in vivo and immunoinformatic approaches, we revealed that the action of the positive selection pressure induces a decrease in virulence and alteration in pathogenicity and antigenicity. However, we also noted that the evolutionary process of CSFV, especially in segregated microenvironments, could contribute to the gain-fitness event, restoring the highly virulent pattern of the circulating strains. Besides, we denoted that the presence of low virulent strains selected by bottleneck effect after inefficient vaccination can lead to a relevant challenge for the epidemiological surveillance of CSF, contributing to under-reports of the disease, favouring the perpetuation of the virus in the field. In this study, B-cell and CTL epitopes on the E2 3D-structure model were also identified. Thus, the current study provides novel and significant insights into variation in virulence, pathogenesis and antigenicity experienced by CSFV strains after the positive selection pressure effect.

Osvaldo Fonseca-Rodriguez and Lester J. Perez contributed equally to this work.

KEYWORDS
antigenicity, classical swine fever virus, pathogenesis, positive selection pressure, surveillance, virulence

1 | INTRODUCTION

Classical swine fever (CSF) is considered one of the most important infectious diseases in animal health (Postel, Austermann-Busch, Petrov, Moennig, & Becher, 2018). The disease is highly contagious and affects both domestic pigs and wild boar (*Sus scrofa*). Due to its devasting consequences in the pig production and tremendous socio-economic impact (Edwards et al., 2000), CSF is notifiable to the World Organisation of Animal Health (OIE; Moennig, Becher, & Beer, 2013).

Classical swine fever is caused by CSF virus (CSFV), a member of the genus *Pestivirus* of the family *Flaviviridae* (Meyers & Thiel, 1996). Consequently, CSFV genome consists of a single plus-strand RNA which contains a single large open reading frame (ORF) flanked by two untranslated regions (UTRs). The ORF encodes a polyprotein of approximately 3,900 amino acids which is subsequently processed into mature proteins by cellular and viral proteases in four structural proteins (C, Erns, E1, E2) and 8 non-structural proteins (Npro, P7, NS2, NS3, NS4A, NS4B, NS5A, NS5B; Meyers & Thiel, 1996). The glycoprotein E2 exposed on the outer surface of the virus is the most immunogenic among all CSFV proteins, inducing neutralizing antibodies and protection against lethal challenge (Wang, Wang, Zhao, Li, & Qiu, 2000).

Based on virulence degrees, CSFV strains can be classified as highly, moderately or low virulent (Weesendorp, Stegeman, & Loeffen, 2009). Depending of the virulence of the CSFV strains, together with host-related factor such as age, breed and immune status, different clinical manifestation of CSF could be presented (Moennig, Floegel-Niesmann, & Greiser-Wilke, 2003). Thus, three main forms of the disease have been defined, acute (transient or lethal), chronic and persistent course, each of them showing a high variability of the clinical signs (Blome, Staubach, Henke, Carlson, & Beer, 2017b).

Despite the global efforts to control and eradicate CSF, the disease remains endemic in several regions around the world including South and Central America, the Caribbean, Asia and some Eastern European countries (Postel et al., 2018). Consequently, the use of lapinized vaccines or live attenuated vaccines has been one of the most common policies to control CSF in endemic countries (Blome, Moss, Reimann, Konig, & Beer, 2017a). However, recent reports have shown the emergence of new CSFV strains resulting from the action of the positive selection pressure, due mainly to bottleneck effects generated by conventional vaccines (thereafter considered as positively selected strains; Hu et al., 2016; Ji, Niu, Si, Ding, & He, 2014; Perez, Diaz de Arce, et al., 2012a; Rios et al., 2017; Shen et al., 2011). All the studies characterizing the action of the positive selection pressure on field CSFV strains, have shown, as a consensus, a decrease in the genetic diversity of the circulating CSFV strains (Hu et al., 2016; Ji et al., 2014; Perez, Diaz de Arce, et al., 2012a; Rios et al., 2017; Shen et al., 2011). However, there is little information about the effect caused by this selective force on the virulence degree, antigenicity and pathogenicity of CSFV strains. In this regard, Perez, Diaz de Arce, et al. (2012a)) observed in one of the positively selected strains studied, a decrease in virulence with the emergence of a low virulent strain from its highly virulent ancestor (Perez, Diaz de Arce, et al., 2012a; Postel et al., 2015), whereas Ji et al. (2014) and Hu et al. (2016) limited their study to analyse the genetic diversity of the strains but speculated about the possibility that the positively selected strain could have alterations in virulence and pathogenesis. Hence, it is still unclear how the positive selection pressure could affect the virulence and pathogenicity of CSFV and the implications of its epidemiological surveillance are far to be completely understood.

The recent boost of the immunoinformatics in scientific research to accurately predict and characterize epitopes (Backert & Kohlbacher, 2015) in combination with classical technics to analyse antigenic metric distances between ancestral and emergent viral strains(Archetti & Horsfall, 1950; Li et al., 2013; Liu et al., 2015) has become indispensable to gain a better understanding in the phenomenon of emergence of mutant viral strains which escape to established vaccines. Accordingly, the current study was aimed to determine the effect of the positive selection pressure on the virulence, pathogenesis and antigenicity of CSFV strains emerged as a result of a bottleneck effect induced by improper vaccination in a CSF-endemic area. In addition, the effect of this type of strains (positively selected strains) on the epidemiological surveillance system was also assessed by spatiotemporal analysis and comparison of reported clinical signs between high- and low-rate clusters.

2 | MATERIALS AND METHODS

2.1 | Cells and viral strains used in the study

Porcine kidney cell line PK-15 cells (ATCC CCL 33) which are widely described as permissive for CSFV were cultured in Dulbecco's Modified Eagle Medium (DMEM), supplemented with 10% foetal bovine serum (FBS; tested pestivirus-free) at 37°C in 5% CO_2. For viral infection, PK-15 cells were infected at a multiplicity of infection (MOI) of 0.1, viruses were harvested 48 hr post-infection. Titrations were performed by end-point dilution using a peroxidase-linked assay (PLA; Wensvoort, Terpstra, Boonstra, Bloemraad, & Zaane, 1986), and titres were calculated according to Reed and Muench (Reed & Muench, 1938).

All the viral strains used in the current study are listed in Table 1. The strain CSFV/Alfort187 was only included for

TABLE 1 Summary of viruses used in this study

Viral strain	Reference No.	Year of isolation	Country	GenBank protein ID	Classification
Margarita	CSF0705	1958	Cuba	AFP86048	Subgenotype 1.4
Holguin[a]	CSF1056	2009	Cuba	AFP86049	Subgenotype 1.4
Santiago de Cuba[a]	CSF1057	2011	Cuba	AFP86050	Subgenotype 1.4
Pinar del Rio[a]	CSF1058	2010	Cuba	AFP86051	Subgenotype 1.4
Alfort/187	CSF0902	1968	France	CAA61161	Subgenotype 1.1

[a]Viral strains emerged by the action of the positive selection pressure induced by a conventional vaccine defined in Perez et al. and confirmed in Rios et al.

comparison purposes, to be used as standard during viral neutralization test (VNT), whereas the remaining four strains, which belong to the subgenotype 1.4 (Postel et al., 2013), were used for the evaluation of virulence, antigenicity and pathogenicity. The strain CSFV/Margarita (CSF0705)/1958 is a highly virulent strain, and it is considered the ancestral viral strain for all the Cuban viral strain (de Arce et al., 2005; Diaz de Arce et al., 1999; Perez, Diaz de Arce, et al., 2012a; Rios et al., 2017), the remaining CSFV strains: CSFV/Holguin(CSF1056)/2009, CSFV/Santiago de Cuba(CSF1057)/2011 and CSFV/Pinar del Rio(CSF1058)/2010 were previously isolated (Perez, Diaz de Arce, et al., 2012a) and classified as positively selected strains (Perez, Diaz de Arce, et al., 2012a; Rios et al., 2017). In a previous study, the strain CSFV/Pinar del Rio(CSF1058)/2010 was described as low virulent (Postel et al., 2015); however, the antigenic relationship of this strain compared to other positively selected strains is completely unknown, therefore, it was included into the current study for this additional assessment.

2.2 | Experimental infection and collection of samples

A total of 23 clinically healthy 6-week-old (Landrace × Large White × Duroc) pigs with similar size were used for experimental infection with the different CSFV strains. All the animals were tested negative to porcine circovirus type 2 (PCV2), porcine parvovirus and suis herpesvirus 1 by real-time RT-PCR (Perez, Perera, et al., 2012b); to porcine reproductive and respiratory syndrome virus (PRRS) by ELISA (IDEXX PRRS X3 Ab Test,); and to other ruminant pestiviruses by multiplex RT-PCR (Diaz de Arce et al., 2009). The animals were randomly divided into five groups and then intranasally inoculated using 2 ml of DMEM (1 ml per nostril) containing 10^5 $TCID_{50}$ ml of the strains: CSFV/Pinar del Rio (CSF1058)/2010 (Group I, pigs # 101, 102, 103, 104, 105), CSFV/Holguin (CSF1056)/2009 (Group II, pigs # 201, 202, 203, 204, 205), CSFV/Santiago de Cuba (CSF1057)/2011 (Group III, pigs # 301, 302, 303, 304, 305), CSFV/Margarita (CSF0705)/1958 (Group IV, pigs # 401, 402, 403) and in the control group each animal was inoculated with 2 ml of DMEM (Group V, pigs # 501, 502, 503, 504, 505). Following infection, rectal temperature and assessment of clinical signs of each pig were recorded daily, the inspection was conducted by a trained veterinarian in a blinded manner.

A semiquantitative judgement of clinical scores (CS) was established based on the parameters previously defined by Tarradas et al. (Tarradas et al., 2014), briefly: the clinical signs were scored from 0 to 7 as follows: 0: no signs; 1: mild pyrexia; 2: pyrexia plus mild clinical signs; 3: mild-moderate clinical signs but no nervous disorders; 4: slight nervous disorders and moderate rest of clinical signs; 5: moderate nervous disorders and moderate–severe rest of clinical signs; 6: severe clinical signs (including nervous disorders); and 7: death. For animal welfare reasons animals that showed a CS of 5 or higher, exhibiting a fall of the hindquarter, inability to get up to drink and prostration or when exhibiting moderate nervous disorders, were euthanized. Serum samples, nasal and rectal swabs were collected at 0, 4, 7, 11, 14, 18 and 21 days post-infection (dpi). After death or euthanasia, animals were subjected to necropsies to assess pathological signs compatible with CSF in different organs and tissues. Finally, tissue samples including tonsils, spleen, lymph nodes and ileum were collected.

2.3 | Isolation, cDNA synthesis and detection by RT-qPCR of viral RNA

Viral RNA was extracted from 140 µl of the sample using a QIAamp Viral RNA Mini Kit (Qiagen GmbH) in accordance with the manufacturer's directions. cDNA synthesis was conducted by random priming, using M-MLV reverse transcriptase as described by Diaz de Arce et al. (2009). Specific CSFV RNA detection in all collected samples was performed by RT-qPCR described by Perez, Arce, Tarradas, et al. (2011b). Results were considered positive when the assay yielded cycle threshold values lower than 35 (Ct < 35). All RT-qPCR experiments were run on a LightCycler 2.0 instrument (Roche Applied Science).

2.4 | Detection of neutralizing antibodies

Virus neutralization test (VNT) was conducted to evaluate the presence of neutralizing antibodies in the serum samples collected. Thus, VNT was performed by neutralization peroxidase-linked assay (NPLA) following standard procedures described in the OIE Manual (OIE, 2014; Terpstra, Bloemraad, & Gielkens, 1984). Finally, titres of neutralizing antibodies (N^A) were expressed as the reciprocal dilution of serum that prevented virus growth for 100 $TCID_{50}$ of the CSFV/Alfort187 strain in 50% of the replicate wells (Terpstra et al., 1984).

2.5 | Antisera production

Antisera specific against each viral strain were obtained as described previously by Coronado et al. (2017) briefly: eight New Zealand White rabbits weighing 2.5 kg were divided into four groups (two animal/group). Each group was inoculated with a viral solution containing $10^{7.2}TCID_{50}$ for each viral strain (CSFV/Pinar del Rio (CSF1058)/2010, CSFV/Holguin (CSF1056)/2009, CSFV/Santiago de Cuba (CSF1057)/2011 and CSFV/Margarita (CSF0705)/1958). Viral solutions were emulsified V/V with Montanide 888 as adjuvant (Seppic). All the animals were subcutaneously immunized (three times with 3-week intervals) in six deposits in the back to guarantee high antibody titres (Perez, Diaz de Arce, Barrera, Castell, & Frias, 2009). Before each inoculation, serum samples were collected from the rabbits via the jugular vein and the antibody titres were monitored using the NPLA assay against the homologous viral strain (Terpstra et al., 1984). After euthanizing the animals (2 weeks after the last inoculation), sera pools from each inoculated group were collected. Antibody titres for each viral strain were expressed as the reciprocal dilution of serum that neutralized 100 $TCID_{50}$ of each homologous strain in 50% of the culture replicates. Finally, the neutralizing titres were calculated using Reed and Muench method (Reed & Muench, 1938).

2.6 | Neutralization capacity induced by the vaccine in use

The capacity to escape to the antibody response induced by the vaccine (strain Labiofam in use for prophylactic vaccination in Cuba; Perez, Diaz de Arce, et al., 2012a) was assessed by neutralization of the anti-Labiofam vaccine pig hyperimmune serum against all the four Cuban CSFV strains (Table 1), as previously described by Coronado et al. (2017) with some modifications, briefly: triplicate heat-inactivated serum with a neutralization titre of 1:50 against CSFV/Alfort187 strain were mixed with equal volumes of all four viral strains including the ancestral CSFV/Margarita (CSF0705)/1958 and the three positively selected strains, CSFV/Pinar del Rio (CSF1058)/2010, CSFV/Holguin (CSF1056)/2009 and CSFV/Santiago de Cuba (CSF1057)/2011. Neutralizing antibody titre was set based on the historical accepted criteria that neutralizing antibody titre higher than 1:32 must be protective against CSFV infection and viral transmission (Terpstra & Wensvoort, 1988). In all cases, the reactions (serum + virus) were incubated at 37°C for 1 hr and subsequently transferred to 96-well plates with PK-15 cells. Peroxidase-linked assay (PLA; Wensvoort et al., 1986) was used for viral titration following the statistical methods described by Reed and Muench (1938).

2.7 | Antigenic distance metric

The antigenic difference between two CSFV viral strains was measured using the Archetti-Horsfall antigenic distance metric (1/*r*) (Archetti & Horsfall, 1950). Archetti-Horsfall antigenic distance metric is independent of the viral receptor binding avidity of any two viruses (X and Y), it requires homologous and heterologous antibody titres for viruses X and Y and it has been widely accepted to classify antigenic differences among different viral agents including, influenza virus (Li et al., 2013), infectious canine hepatitis virus (Kinjo & Yanagawa, 1968), infectious bronchitis virus (Dolz, Pujols, Ordonez, Porta, & Majo, 2008) and others (Liu et al., 2017).

The antigenic distance metric for the CSFV strains was estimated using the following equation (1). Antigenic distances resulting $0.5 < (1/r) < 1.5$ indicate no significant antigenic difference between the two viruses, results of $1.5 < (1/r) < 2$ indicates antigenic difference between the two viruses, whereas $(1/r) \geq 2$ means that the two virus strains present major antigenic difference (Archetti & Horsfall, 1950; Liu et al., 2017).

$$r = \sqrt{\frac{N^{BA} \times N^{AB}}{N^{AA} \times N^{BB}}} \quad (1)$$

N^{AA} and N^{BB} (homologous neutralizing titres of two strains), N^{BA} and N^{AB} (heterologous neutralizing titres against each other).

2.8 | Epitope characterization by immunoinformatics approach

The main objective of the immunoinformatics is to convert and organize large-scale immunological data combining statistical and machine learning systems, to obtain immunologically meaningful interpretations (Soria-Guerra, Nieto-Gomez, Govea-Alonso, & Rosales-Mendoza, 2015). The proper use of immunoinformatics tools has shown a high degree of accuracy; therefore, this discipline has been employed to characterize molecular interactions between epitopes defining new hypotheses related to understand the immune system mechanisms (Wang et al., 2016), as well as to develop new multi-epitope vaccine strategies against emergent viral diseases such as Zika virus (Dikhit et al., 2016; Pradhan et al., 2017), and Ebola virus (Dikhit et al., 2015), or re-emerging viruses: Hepatitis C virus (Ashraf, Bilal, Mahmood, Hussain, & Mehboob, 2016) and Dengue virus (Ali et al., 2017). In this study, we used immunoinformatics approach to characterize both T-cell and B-cell epitopes for the main immunogenic protein of CSFV (E2 protein). This characterization can facilitate the understanding of how the positively selected CSFV strain could escape to both cellular and humoral immune responses elicited by the vaccine. To determine the presence of T-cell epitopes, B-cell epitopes, CTL epitopes, MHC-I binding and deimmunization properties, the E2 protein sequence from the CSFV/Margarita (CSF0705)/1958 strain was used. The variation caused on all the epitopes found was evaluated using the E2 protein sequences from the positively selected strains.

2.8.1 | B-cell epitope prediction

Linear B-cell epitopes for E2 protein of CSFV were predicted following the methodology recently described by Narula, Pandey,

TABLE 2 Predicted B-cell epitopes for E2 protein of CSFV

S.No	Peptide(*) position	BCPred	AAP	FBCPred	Antigenicity prediction
1	^{24}E(*GLTTTWKDYDHNLQ*)LDDGTIKA^{47a}	0.760	0.989	0.867	0.6520
2	^{78}VTFE(*LFDGTSPSIEEMGDD*)FGFGLGLCPF^{107a}	0.993	1.000	0.997	0.5886
3	^{102}LCPFDTSPVVK(*GRYNTTLLNGS*)AFY^{127a}	0.993	1.000	0.970	0.6994
4	^{135}GVIE(*CTAVSPTTLRTE*)VVKTFRRE^{159a}	0.983	1.000	1.000	0.8889
5	^{181}RL(*GGNWTCVKGEPVIY*)TGGLV^{202}	0.777	1.000	0.998	0.6484
6	^{204}CRWCGFDFN(*EPDGLPHYPIG*)KCILANETG^{233}	0.873	1.000	0.997	0.2401$^{N.A}$
7	^{269}LDERLGPM(*PCRPKE*)IVSSEGPVRKTSCT^{297}	0.995	1.000	0.978	0.6981

Note: Values represent the score obtained from the prediction of the preferences of B-cell epitopes based on three different algorithms BCPred (El-Manzalawy et al., 2008b), APP (Chen et al., 2007) FBCpred (El-Manzalawy et al., 2008a) and the level of antigenicity for each epitope predicted by VaxiJen (Doytchinova & Flower, 2007). BCPred, AAP and FBCPred threshold values were set to 75% level of specificity to guaranty the higher level of accuracy, for antigenicity prediction the threshold was set at 0.5 to guarantee the highest values for sensitivity (94%), specificity (84%) and accuracy (89%) for more detail see Doytchinova and Flower (2007).
Abbreviation: N.A, non-antigenic.
[a]B-cell epitopes for E2 protein of CSFV also recognized by T-cell epitopes and TCD4+ (see Table S5)
*Common mer for the three methods used (the complete list of B-cell found for each method is presented is Table S1).

Khatoon, Mishra, and Prajapati (2018) with some modifications: BCPREDS server freely available (http://ailab.ist.psu.edu/bcpred/) (El-Manzalawy, Dobbs, & Honavar, 2008a) was used to predict the linear B-cell epitopes based on the three prediction methods: AAP method (Chen, Liu, Yang, & Chou, 2007), BCPred (El-Manzalawy, Dobbs, & Honavar, 2008b) and FBCPred (El-Manzalawy et al., 2008a). In all cases, default parameters were used. For this study, only the results that yielded overlapping regions from the three methods were considered (Table 2 and Table S1). Finally, the epitopes selected were further analysed using VaxiJen (Doytchinova & Flower, 2007) to evaluate antigenicity using a threshold = 0.5.

2.8.2 | T-Cell epitope prediction

Since T-cell epitopes are bound in a linear form to MHCs, the interface between ligands and T cells can be modelled with accuracy. Thus, the current predictor tools to identify putative T-cell epitopes MHC-I binding are very efficient and have wide allelic coverage, with an estimated accuracy in the range of 90%–95% positive prediction value (Soria-Guerra et al., 2015). To identify the T-cell epitopes for E2 protein of CSFV with higher accuracy, we established the following strategy: (a) we mapped the promising epitopes using IEDB 2.19 methodology (Recommended) of IEDB Analysis Resource (Lundegaard et al., 2008; Nielsen et al., 2003) (http://tools.iedb.org/mhci/) for pig species, restricted to the Swine Leukocyte Antigen (SLA) alleles: SLA-1*0101, SLA-1*1101, SLA-1*1301 SLA-2*0101, SLA-3*0101, SLA-3*0602. The restriction for SLA haplotypes was based on two criteria: the alleles present in the swine breeds *Large White* and *Landrace* (Sorensen et al., 2017), both present in Cuban pig population (Rios et al., 2017), and the SLA alleles identified which specifically bind different CTL epitopes of CSFV (Gao et al., 2017). The cut-off score was set to IEDB ≤1 to guarantee maximum epitope-like properties (Table S2; Lundegaard et al., 2008; Nielsen et al., 2003), for the prediction of T-cell epitopes other software such as SYFPEITHI or BIMAS were not used since in these programs, predictions for alleles from pig are not available; (b) a search for MHC-I binding was also performed using NetMHC 4.0 Server. Prediction of peptide-MHC class I which uses an artificial neural networks (ANNs) algorithm (Andreatta & Nielsen, 2016; Nielsen et al., 2003), thresholds for strong and weak binding were set to 0.5 and 2, respectively, predicted peptides with score values above 2 were not considered (Table3). Finally, peptides predicted by both programs were selected and kept for further analysis (Table 3).

2.8.3 | CTL and T-CD4+ epitope predictions

CTL epitopes of E2 protein of CSFV were predicted using NetCTLpan 1.1 Server (http://www.cbs.dtu.dk/services/NetCTLpan/; Stranzl, Larsen, Lundegaard, & Nielsen, 2010). This method integrates prediction of peptide-MHC class I binding, proteasomal C terminal cleavage and TAP (Transporter Associated with Antigen Processing) efficiency. MHC class I binding predictions are performed using artificial neural networks. The proteasome cleavage event is predicted using the version of the NetChop neural networks trained on C terminals of known CTL epitopes as described for the NetChop-3.0 server, and TAP transport efficiency is predicted using the weight matrix-based method described by Peters et al. (Peters, Bulik, Tampe, Endert, & Holzhutter, 2003). The prediction threshold values were set by default, and the search was accomplished for 8, 9, 10 and 11-mer peptides (Table S4). T-CD4+ epitope prediction was conducted using CD4-T-cell immunogenicity prediction from IEDB Analysis Resource (Lundegaard et al., 2008; Nielsen et al., 2003; http://tools.iedb.org/mhci/) with IEDB as prediction method and a percentile rank threshold = 50 was used (Table S5). Only those CTL epitopes and T-CD4+ epitopes overlapping, previously confirmed as T-cell epitopes (Section 2.9.22.8.3) were considered (Table 4).

TABLE 3 Predicted T-cell epitopes for CSFV E2 proteins overlapping with MHC-I binding prediction

S.No	SLA haplotype	Peptide(*) position	IEDB[a]	MHC-I[b]
1	SLA-1*1101	^{18}IGQLGAEGL^{26}	0.57	1.4
2	SLA-1*1101; SLA-3*0602; SLA-1*1301; SLA-2*0101	^{44}IKAICTAGSF^{53}	0.28	0.7
3	SLA-1*1301	^{57}ALNVVSRRY^{65}	0.49	0.6
4	SLA-3*0101; SLA-3*0602	^{63}R(RYLASLHK)GAL^{74}	0.19	0.7
5	SLA-1*1101	^{72}GALPTSVTF^{80}	0.58	2
6	SLA-1*1101; SLA-2*0101; SLA-1*1301	^{76}TSVTFELLF^{84}	0.17	1
7	SLA-1*1301; SLA-1*0101	^{83}LFDGTSPSI^{91}	0.64	1.1
8	SLA-1*1301	^{90}SIEEMGDDF^{98}	0.16	0.4
9	SLA-3*0602; SLA-3*0101; SLA-1*1101	^{112}KGRYNTTLL^{120}	0.09	1.1
10	SLA-1*0101; SLA-1*1301; SLA-1*1101; SLA-2*0101; SLA-3*0602; SLA-3*0101	^{113}GRYN(TTLLNGSAFY)L^{127}	0.09	0.5
11	SLA-1*1101; SLA-1*0101; SLA-2*0101; SLA-3*0101; SLA-3*0602	^{123}SAFYLVCPI^{131}	0.09	1.7
12	SLA-1*1101; SLA-2*0101; SLA-3*0101; SLA-3*0602	^{153}KTFRREKPF^{161}	0.88	0.01
13	SLA-1*0101; SLA-1*1101;SLA-1*1301; SLA-2*0101	^{170}T(TVENEDLFY)^{179}	0.11	0.03
14	SLA-3*0602; SLA-3*0101	^{202}KQCRWCGFDF^{211}	0.46	0.9
15	SLA-1*1301	^{208}GFDFNEPDGLPHY^{220}	0.86	1
16	SLA-1*1301; SLA-1*0101	^{225}(CILANETGY)RI^{235}	0.68	0.07
17	SLA-1*0101	^{238}STDCNRNGV^{246}	0.09	0.25
18	SLA-1*1301; SLA-1*0101	^{267}ALDERLGPM^{275}	0.65	0.5
19	SLA-3*0602; SLA-3*0101; SLA-2*0101	^{289}V(RKTSCTFNY)TKTLR^{303}	0.29	0.03
20	SLA-1*1301; SLA-3*0602; SLA-2*0101	^{300}KTLRN(KYYEPRDSYF)^{314}	0.25	0.5
21	SLA-3*0602; SLA-3*0101	^{310}RDSYFQQYML^{319}	0.26	2
22	SLA-1*1301; SLA-2*0101	^{316}Q(YMLKGEYQY)W^{326}	0.07	0.7
23	SLA-3*0101; SLA-3*0602; SLA-1*1101; SLA-1*0101	^{320}KGEYQYWFDLDV^{331}	0.3	0.7
24	SLA-1*1301	^{326}W(FDLDVTDHHSDYF)^{339}	0.5	0.8
25	SLA-1*1301; SLA-1*0101; SLA-1*1101	^{330}D(VTDHHSDYF)TEF^{342}	0.02	0.06
26	SLA-1*0101; SLA-1*1101; SLA-1*1301; SLA-3*0101; SLA-3*0602	^{334}H(HSDYFTEFL)VL^{345}	0.06	1.2

Note: Scores for the predictive values of T-cell epitopes and MHC-I bindings restricted to the Swine Leukocyte Antigen (SLA) alleles: SLA-1*0101, SLA-1*1101, SLA-1*1301 SLA-2*0101, SLA-3*0101, SLA-3*0602.

[a]Threshold value was set to IEDB ≤1 to guarantee maximum epitope-like properties.

[b]Threshold value was set to NetMHC 4.0 Server Prediction (MHC-I binding) ≤2 to guarantee maximum binding level. In all cases, lower percentile rank = better binders.

*lower mer for the peptide.

2.8.4 | Deimmunization prediction

The deimmunization prediction tool has been recently created to identify immunodominant regions and predict those amino acid substitutions that create non-immunogenic versions of the proteins (Dhanda et al., 2018). The tool also predicts whether the action of substitution on the immunogenic peptides could create alteration in immunogenic sites in the neighbouring peptides (Dhanda et al., 2018). Thus, to assess the role of mutations on different sites of E2 protein of the positively selected strains in comparison with the ancestral CSFV strain, we performed a search for deimmunization for the E2 protein using http://tools.iedb.org/deimmunization/ an default parameters. For interpretation of the results, we used the guides at deimmunization score http://tools.iedb.org/deimmunization/help/

2.8.5 | 3D structure representations

The structural model for E2 protein of CSFV previously obtained by our research group in Rios et al. (2017) was used to represent the mutations involved in the escape to the immune response of the host induced by the vaccine on B-cell epitopes, T-cell epitopes and CTL epitopes. Mutations inducing deimmunization alterations on immunogenic sites and neighbouring peptides were also represented. Pymol software package (Schrodinger, 2015) was used to visualize 3D crystal structures of the E2 protein.

TABLE 4 Predicted Cytotoxic T-lymphocyte (CTL) epitopes for E2 protein of CSFV

S.No	Allele	Peptide position (*)	Rank
1	SLA-1*0201; SLA-2*0101	^{1}RLACKEDFRY^{10a}	0.80
2	SLA-1*0201; SLA-2*0101	^{26}LTTTWKDY^{34}	0.80
3	SLA-1*0201; SLA-1*1301; SLA-2*0101; SLA-3*0602	^{55}VIALNVVSRRY^{66a}	0.80
4	SLA-1*0101; SLA-1*0201; SLA-1*1101; SLA-1*1301; SLA-2*0101; SLA-3*0101; SLA-3*0602	^{72}GALPTSVTFELLF^{85a}	0.20
5	SLA-1*1101	^{98}FGFGLCPF^{106}	0.80
6	SLA-1*0201; SLA-1*1301; SLA-2*0101; SLA-3*0602	^{116}NTTLLNGSAFYL^{128a}	0.15
7	SLA-1*0201; SLA-2*0101	^{169}TTTVENEDLFY^{180}	0.80
8	SLA-1*0201	^{226}ILANETGY^{234a}	0.80
9	SLA-1*0201; SLA-1*1301; SLA-2*0101; SLA-3*0602	^{291}KTSCTFNY^{299a}	0.15
10	SLA-2*0101; SLA-3*0101; SLA-3*0602	^{300}(KTLRNKYY) EPRDSYF^{315a}	0.15
12	SLA-1*0201; SLA-1*0101; SLA-1*1101; SLA-1*1301; SLA-2*0101; SLA-3*0101;SLA-3*0602	^{312}SYFQQ(YMLKGEYQY WFDL)^{330}	0.10
14	SLA-1*0201	^{331}(VTDHHSDY)FTEF^{343a}	0.80
16	SLA-1*0201; SLA-1*1101; SLA-1*1301; SLA-2*0101; SLA-3*0602	^{346}V(VVALLGGRYVL) WLIVT^{362a}	0.20

Note: Rank = Scores for the predictive values of CTL epitopes calculated as a weighted average of the major histocompatibility complex class I molecules (MHC-I Prediction score), transporter associated with antigen processing (TAP score) and C terminal cleavage scores, for more details see: Stranzl et al. (2010).

[a]CTL epitopes also recognized as TCD4+ epitopes (TCD4+ are shown in Table S5). Threshold values were set by default at as follow: weight on C terminal cleavage = 0.225, weight on TAP transport efficiency = 0.025 and threshold for epitope identification = 1.0.

*lower mer for the peptide.

2.9 | Statistical analysis

Results are expressed as mean ± standard error of the mean. Statistical analyses were performed using Prism v6 software (GraphPad). Pairwise comparisons between groups were performed using unpaired two-tailed Student's *t* test and comparisons between multiple groups were performed using one-way or two-way analysis of variance (ANOVA) followed by a Tukey or Sidak post hoc test, as appropriate. Differences were determined as statistically significant at $p < .05$.

2.10 | Spatiotemporal analysis and clinical signs comparison between high- and low-rate clusters of secondary data

Cuba is an endemic country to CSF, where both spatial segregation and the selection pressure exerted by the vaccine seem to drive the evolutionary pattern of a CSFV lineage positively selected (Rios et al., 2017), which makes it an attractive scenario to get a better understanding of how the emergence of positively selected strains can impact the epidemiological surveillance systems. For this purpose, a spatiotemporal analysis and a clinical signs comparison between high- and low-rate clusters of secondary data at national level were conducted.

All the information was collected from the National Laboratory for Veterinary Diagnostic (NLVD). National Laboratory for Veterinary Diagnostic is responsible for the CSF primary diagnostic in the Republic of Cuba. All CSF-suspected samples from all the regions of the country are submitted to NVLD for confirmatory diagnostic by Direct Immunoperoxidase (IPD) technique. Thus, NVLD reports a confirmed CSF-case if at least one of the animals tested yields a positive result to IPD in the suspected premise.

The information available included: (a) CSF-confirmed positive pig holdings from 2010 to 2016, (b) epidemiological questionnaire from investigated premises. The information from the affected pig holdings contained: farmer name, province, municipality, data of case confirmation, geographical location using the epidemiological quadrant of 1 km^2 according to National Surveillance Epizootiological System, and clinical signs reported by trained veterinary staff.

A space–time permutation model implemented in SaTScan 9.3 (Kulldorff, 2014) was used to detect high- and low-rate spatiotemporal clustering. A circular scanning window, set to contain a maximum

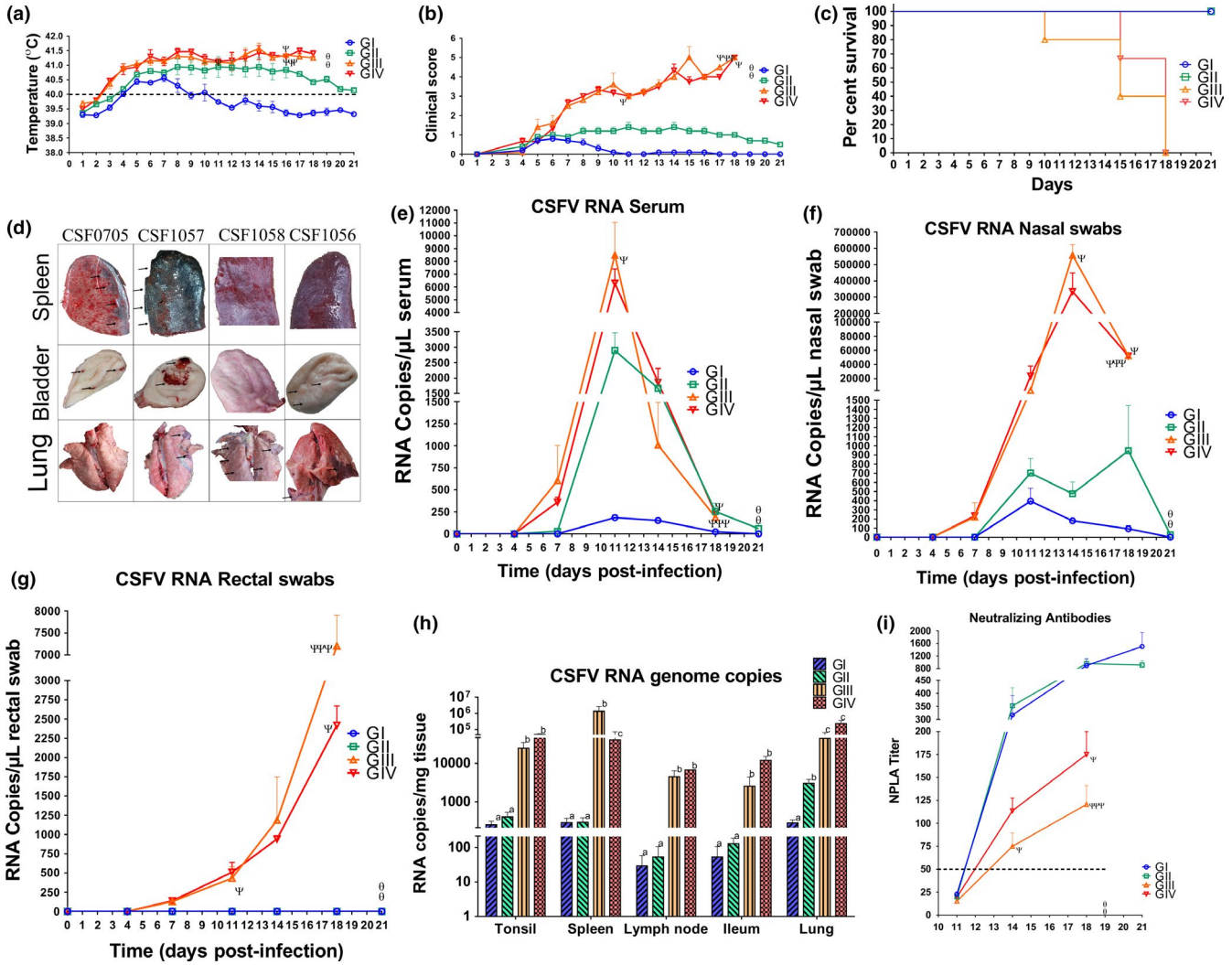

FIGURE 1 Evaluation of virulence and pathogenesis for the four studied CSFV strains including the three strains selected by the action of the positive selection pressure and their ancestral highly virulent strain. (a) Rectal temperatures of the pigs after the challenge with CSFV strains, daily mean and standard deviation of the temperature per group is shown, fever was considered as rectal temperature >40°C. (b) Clinical scores after CSFV infection. (c) Survival curves of the challenged pigs, different curves indicated different groups. (d) Representative pathologic lesions in the pigs inoculated with CSFV/Margarita (CSF0705)/1958 (denoted as CSF0705), CSFV/Santiago de Cuba (CSF1057)/2011 (denoted as CSF1057), CSFV/Holguin (CSF1056)/2009 (denoted as CSF1056) and CSFV/Pinar del Rio (CSF1058)/2010 denoted (CSF1058) (lesions are denoted with black arrows). Quantification of viral RNA in the CSFV- challenged pigs in (e) serum samples, (f) nasal swab samples, (g) rectal swab samples and (h) in major susceptible tissues including: tonsil, spleen, mediastinal lymph node (denoted as lymph node), ileum and lung, bars indicate the means of CSFV-RNA load, standard deviation are also represented, different letters indicate significant differences by two-way analysis of variance (ANOVA) followed by a Tukey or Sidak post hoc test at $p < 0.05$. In all cases, the groups are denoted (GI: pigs challenged using the CSFV/Pinar del Rio (CSF1058)/2010 strain, GII: pigs challenged using the CSFV/Holguin (CSF1056)/2009 strain, GIII: pigs challenged using the CSFV/Santiago de Cuba (CSF1057)/2011 strain and GIV: pigs challenged using the CSFV/Margarita (CSF0705)/1958 strain), samples that were not taken by consequence of the animal sudden death or euthanized were also denoted (ψ) or (θ) when all the animals from the group were already dead or euthanized. (i) Time-course of CSFV-specific neutralizing antibody response after the CSFV-challenge trial in pigs, mean and standard deviation values obtained by NPLA assay is shown, all the groups are denoted, the value of neutralizing antibody 1:50 commonly reported as protective is also denoted [Colour figure can be viewed at wileyonlinelibrary.com]

of 50% of the study region surface and 50% of the study period, was used. Identified clusters were considered significant at $p < .05$, based on Monte Carlo hypothesis testing with 9,999 permutations. Detected clusters were geographically represented using ArcGIS 9.3.1 (ESRI, 2009).

The frequency of clinical signs reported in the observed holdings from high-rate clusters (holding of pig affected during the cluster period) was compared with the affected pig holdings that belonged to the low-rate clusters. The clinical signs reported were (a) loss of appetite, (b) fever, (c) conjunctivitis, (d) diarrhoea, (e) lack of coordination, (f) cyanosis/petechial haemorrhages, (g) neurological signs, (h) respiratory signs, (i) poor growth, (j) abortions and stillbirths and (k) mummification and malformations. A comparison was made by the univariate analysis of the variables (clinical signs) using Fisher's exact

test to determine if significant differences ($p < .05$) exist between affected pig holdings on high-rate and low-rate clusters. The odds ratio (OR) and 95% confidence intervals were computed and provided. The statistical calculations were carried out using R software.

3 | RESULTS

3.1 | Virulence and pathogenesis of positively selected CSFV strains

3.1.1 | Clinical signs developed in the infected pigs

The obtention of detailed information about the milder forms of CSFV as well as in vivo comparison of the parameters of CSFV of different virulence in pigs has become a current need for the scientific community (Wang et al., 2018; Zhang et al., 2018). Thus, the virulence and pathogenesis analyses of the three emergent strains in comparison with the ancestral strain showed that all the infected animals from Groups III and IV developed pyrexia (rectal temperature higher than 40°C) starting at 3 dpi and lasting until 18 dpi (Figure 1a), reaching peaks of fever near 41.5°C in some cases (Figure 1a). Animals from Group II also developed pyrexia, but it was delayed 1 day in comparison with animals from Groups III and IV (Figure 1a) and lasted until the end of the experiment. Conversely, the animals from Group I only develop fever for a short period of time during 4 dpi and 10 dpi (Figure 1a).

Animals from Group III and IV displayed moderate and severe clinical signs compatible with CSF starting at 8 dpi until 18 dpi. The clinical signs included anorexia, conjunctivitis, diarrhoea, cough, lameness, abdominal petechiae and nervous disorders. Clinical scores values equal or higher than 4 for both groups were obtained (Figure 1b). It is important to denote that one of the animals from Group III (#303) experienced sudden death at 10 dpi (Figure 1c), whereas other two animals from this same group (#301 and #302) and one animal from Group IV (#401) also experienced sudden death but at 15 dpi (Figure 1c). The remaining animals from these two groups were euthanized for ethical reasons at 18 dpi (Figure 1c). Meanwhile, animals from Group II only experienced pyrexia plus some mild clinical signs no compatible with CSF between 4 and 21 dpi, resulting in a clinical score of around 2 (Figure 1b); and animals from Group I showed no clinical sings aside from the pyrexia devolved during 4 dpi and 10 dpi, resulting in a clinical score equal to 1 during this period of time and thereafter the animals resembled a healthy status with a clinical score equal to 0 (Figure 1b). None of the animals from these two groups experienced sudden death or were euthanized during the study (Figure 1c). The post-mortem examination of animals in Groups III and IV exhibited the presence of pathological lesions compatible with typical or acute CSF infection, including: spleen infarcts (Figure 1d), extensive petechiae in the bladder (Figure 1d) and kidney, necrosis in the tonsils, marginal, haemorrhagic mesenteric and mediastinal lymph nodes, enteritis and pulmonary oedema (data not shown). In the animals examined from Group II, only petechiae in bladders (Figure 1d) was found, no other lesions suggesting CSF infection were present. None of the animals from Group I showed pathological lesions compatible with CSF, the main pathological change observed in some of the animal was the presence of interstitial pneumonia in lungs. The pathological lesions found were further confirmed by haematoxylin/eosin stains on histological sections (Figure S1). Nonetheless, viral RNA (CSFV) was detected in all the animals from the different groups, confirming the infection of these animals with CSFV (Figure 1e–h).

3.1.2 | Dynamic of viral infection and virus shedding

Viral RNA loads determined by RT-qPCR showed that in Groups III and IV viremia for CSFV was detected at 7 dpi, with a viral RNA load of about $10^{2.6}$ for Group IV and $10^{2.9}$ copies/μl for Group III, reaching a maximum at 11 dpi with loads of $10^{3.8}$ and $10^{3.9}$ copies/μl for each group, respectively (Figure 1e). After these peaks of viremia, a reduction in the viral RNA load in serum at 14 dpi was experienced by the animals in both groups. When the animals in these two groups were euthanized at 18 dpi, the viral RNA loads in serum were detected in the order of $10^{2.3}$ copies/μl (Figure 1e). In comparison with Groups III and IV, viremia in Groups I and II was delayed (Figure 1e). The first quantifiable viral RNA loads for both groups were detected at 11 dpi but denoted differences were observed between them, with values in the order of $10^{3.5}$ copies/μl for Group II and $10^{2.4}$ copies/μl for the animals in Group I (Figure 1e). Like the animals in Group III and IV, after reaching a maximum at 11 dpi, the animals in Group I and II showed a slight decline in the viral RNA load in serum but in both cases resembling a plateau, with values in the order of $10^{3.2}$ copies/μl for Group II and $10^{2.3}$ copies/μl for the animals in Group I (Figure 1e). In Group I at 18 dpi only one animal was viremic with a viral load of about 10^{2} copies/μl, whereas in Group II all the animals still presented RNA loads in serum with values of about $10^{2.4}$ copies/μl. However, at the end of the experiment (21 dpi) the CSFV RNA in serum was undetected in almost all animals in both groups, excepting one animal (#203) in Group II that still yielded quantifiable RNA load in serum ($10^{2.4}$ copies/μl) with the longest viremia detected in the study (Figure 1e).

Viral excretion in nasal swabs was detected in Groups III and IV coinciding with the start of the viremia at 7 dpi with viral RNA loads of about $10^{2.3}$ copies/μl (Figure 1f). In both groups, the animals experienced an increase in virus excreted via nasal until 14 dpi with peaks of viral RNA loads of approximately $10^{5.7}$ copies/μl for the animals infected with the strain CSFV/Santiago de Cuba (CSF1057)/2011 (Group III) and $10^{5.47}$ copies/μl for the animals infected with the ancestral and highly virulent strain CSFV/Margarita (CSF0705)/1958 (Group IV; Figure 1f). At the time that the animals in these two groups were euthanized at 18 dpi, a decrease in viral excretion via nasal fluid was observed. However, it is important to denote that the viral RNA load could be considered high, reaching values of $10^{3.63}$ copies/μl (Figure 1f). In Groups I and II, viral excretion in nasal swabs also coincided with the start of the viremia for these two groups at 11 dpi, with values of viral RNA loads of about $10^{2.6}$ copies/μl for Group I and $10^{2.9}$ copies/μl for Group II (Figure 1f). However, the animals from these groups showed a different pattern of excretion compared to the animals in Groups III

and IV, since a significant increase in excretion after the starting point was not observed (Figure 1f). Indeed, the pattern of excretion in nasal secretion in Group I was similar to the pattern obtained in the evaluation of the viremia for this group, but the amount of virus excreted through this via yielded higher values compared to those detected in serum (Figure 1e,f). In fact, at 18 dpi the RNA loads in Group I were still reaching values of 10^2 copies/μl (Figure 1f), evidencing that the animals infected with the strain CSFV/Pinar del Rio (CSF1058)/2010 can excrete considerable amounts of CSFV via nasal secretions without showing any clinical signs or pathological lesions compatible with the disease. Meanwhile in Group II, two peaks of excretion via nasal secretions were observed, one at 11 dpi and the second one at 18 dpi, with values of RNA loads of $10^{2.7}$ copies/μl and $10^{2.9}$ copies/μl, respectively, suggesting an intermitting pattern of excretion for the animals infected with the strain CSFV/Holguin (CSF1056)/2009 (Figure 1f). Like in the evaluation of the viremia pattern, at the end of the experiment (21 dpi), the CSFV RNA in nasal fluid was undetected in almost all the animals in both groups, with the exception once again, of animal #203 in Group II that still yielded quantifiable RNA load ($10^{2.1}$ copies/μl).

An interesting pattern of excretion determined by rectal swab analyses was observed for the animals in Groups III and IV, which showed an exponential increase in the viral RNA load in this type of samples, during the complete experiment for these two groups (Figure 1g). The rectal excretion showed by these two groups started at 7 dpi with viral RNA load values around 10^2 copies/μl and reached the maximum peak at 18 dpi with values of $10^{3.9}$ copies/μl for animals of Group III and $10^{3.4}$ copies/μl for animals of Group IV. Conversely, the animals in Groups I and II did not yield positive results by RT-qPCR to this type of sample throughout the study (Figure 1g). Thus, it could be inferred that the strains CSFV/Pinar del Rio (CSF1058)/2010 and CSFV/Holguin (CSF1056)/2009 are not excreted via faeces, evidencing also a different tropism and virus shedding among all the strains assessed.

According to the level of viremia and excretion displayed, the animals infected with the strains CSFV/Santiago de Cuba (CSF1057)/2011 and CSFV/Margarita (CSF0705)/1958 had a significantly higher viral load compared to those infected with the strains CSFV/Pinar del Rio (CSF1058)/2010 and CSFV/Holguin (CSF1056)/2009 in all the tissue samples assessed including tonsil, spleen, lung, tonsil, mediastinal lymph nodes and ileum (Figure 1h).

3.1.3 | Kinetic of neutralizing antibodies

Neutralizing antibodies were detected in all infected pigs from all the CSFV-infected groups as early as 11 dpi (Figure 1i), matching with the maximum peak of viremia (Figure 1e,i). At 14 dpi all the pigs assessed showed neutralizing antibodies higher than 1:50, but in Groups I and II the titres reached values around 1:300 and 1:350, respectively (Figure 1i). The titres of neutralizing antibodies from the animals in Group I yielded a maximum 1:1,400 and in Group II 1:800 at 21 dpi, whereas the titres of neutralizing antibodies for the remaining groups (III and IV) showed lower values, reaching only 1:100 (Group III) and 1:200 (Group IV; Figure 1i).

3.2 | Evaluation of antigenic variability

3.2.1 | Antigenic relatedness analyses

To study the neutralizing capacity induced by the commercial vaccine in use in Cuba (Labiofam), hyperimmune pig sera generated from the CSFV strain vaccine Labiofam were used to neutralize the ancestral highly virulent Cuban CSFV strain (CSFV/Margarita (CSF0705)/1958) and the three positively selected stains (Table S6). Whereas the three pig sera obtained completely or nearly completely neutralized the CSFV/Margarita (CSF0705)/1958 strain, reducing the viral titre between 4 log and 5 log (Figure 2), a different outcome against the three positively selected strains was observed, evidencing significant differences in the capacity of neutralization of the vaccine in use between the ancestral Cuban CSFV strain and the new emergent strains (Figure 2). Thus, against the strain CSFV/Santiago de Cuba (CSF1057)/2011, the hyperimmune sera showed a partial capacity of neutralization reducing the viral titre only between 2.2 log and 3 log (Table S6 and Figure 2), against the strain CSFV/Holguin (CSF1056)/2009, the hyperimmune sera showed a lower capacity of neutralization reducing the viral titre only between 1.2 log and 2 log (Table S6 and Figure 2), and against the strain CSFV/Pinar del Rio (CSF1058)/2010, hyperimmune sera failed to neutralize this strain or only reduced between 0.2 log and 1.5 log (Table S6 and Figure 2). These results strongly evidence the capacity of escaping of the positively selected strain included in the current work to the humoral response induced by the vaccine in use in Cuba.

To evaluate the antigenic diversity of different CSFV strains a cross-viral neutralization test was performed to calculate the (1/r) value (Table S7). The (1/r) values between ancestral strain CSFV/Margarita (CSF0705)/1958 and two of the positively selected, CSFV/Holguin (CSF1056)/2009 and CSFV/Santiago de Cuba (CSF1057)/2011, were less than 2 but higher than 1.5 (Table 5), indicating antigenic differences between these viral strains. However, no significant antigenic difference was observed between ancestral strain CSFV/Margarita (CSF0705)/1958 and the emergent strain CSFV/Pinar del Rio (CSF1058)/2010 as evidenced by the (1/r) value equal to 0.77. However, a different scenario was observed when the emergent strains were compared between them. Thus, significant major antigenic differences existed between the strain CSFV/Pinar del Rio (CSF1058)/2010 and the other two positively selected strains CSFV/Holguin (CSF1056)/2009 and CSFV/Santiago de Cuba (CSF1057)/2011 with (1/r) values equal to 2 (Table 5). Whereas these last two strains showed antigenic differences with (1/r) value equal to 1.84 (Table 5).

3.2.2 | Characterization of T-cell, CTL and B-cell epitopes for E2 protein of CSFV

To get a better understanding of the results obtained about the antigenic relationships of the CSFV strains, a complete characterization for the T-cell epitopes, MHC-I binding, B-cell epitopes and deimmunization properties, was conducted using immunoinformatic

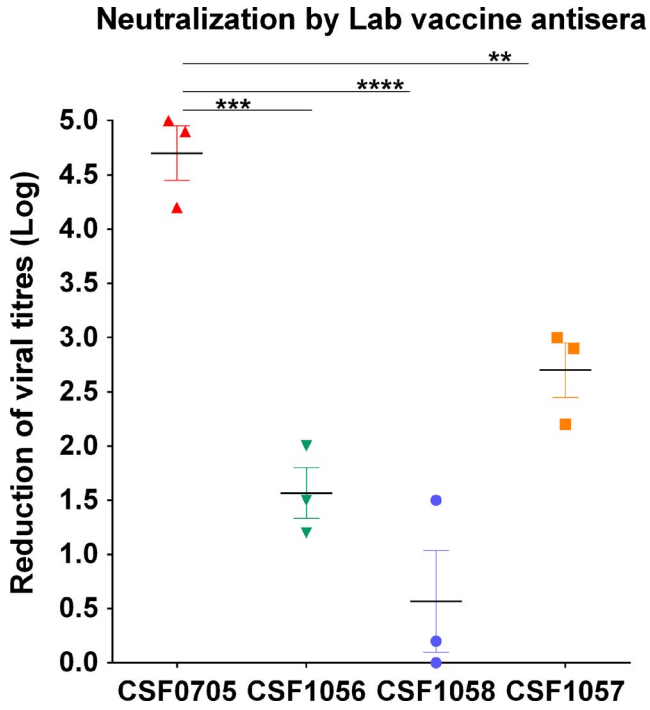

FIGURE 2 Neutralization capacity of hyperimmune pig sera against the ancestral highly pathogenic Cuban CSFV-strain and the three positively selected strains used in the current study. Comparison of the neutralization capacity of the hyperimmune sera is shown as the reduction of the viral titre (Log), the values obtained from each serum is represented, mean of viral titre reduction and standard deviation are also shown, the strain CSFV/Margarita (CSF0705)/1958 was denoted as CSF0705, the strain CSFV/Santiago de Cuba (CSF1057)/2011 was denoted as CSF1057, the strain CSFV/Holguin (CSF1056)/2009 was denoted as CSF1056, and the strain CSFV/Pinar del Rio (CSF1058)/2010 was denoted as CSF1058. Significant differences from a one-way analysis of variance (ANOVA) followed by a Holm–Sidak post hoc test at $p < .05$ (*), $p < .01$ (**). $p < .001$ (***) and $p < .0001$ (****) were also denoted. (A more extensive analysis including also the initial and final viral titres form the different viral strains is shown in Table S6) [Colour figure can be viewed at wileyonlinelibrary.com]

approaches. From the whole repertory of T-cell epitopes detected by IEDB analysis resource for the alleles SLA-1*0101, SLA-1*1101, SLA-1*1301 SLA-2*0101, SLA-3*0101, SLA-3*0602 (Table S4), those that did not showed a potential binding capacity to MHC-I were discarded from the analysis. Thus, a total of 26 T-cell epitopes with different MHC-I binding potential (strong, medium and weak) were selected (Table 3). Since the immune response from both CTL (cellular adaptive immune response) and B-cell (antibody immune response) requires the activation of T cell, the T-cell epitopes were also used to filter the B-cell epitopes and CTL epitopes detected.

Initially, 16 CTL epitopes were detected for E2 protein of CSFV (Table 4). From this pool of epitopes, a total of nine overlapping CTL and TCD4+ epitopes were finally considered as CTL epitopes in our analysis (Table 4). Since the cytotoxic T lymphocyte (CTL) plays an important role in the control and clearance of viral infections (Stipp, Iniguez, Wan, & Wodarz, 2016), those mechanisms driving the evasion of the CTL response could facilitate the perpetuity of the virus into the host. Therefore, we focused on the amino acid changes of the immunogenic E2 protein of the emergent strains in the current study that could induce alterations on the CTL epitopes detected. Thus, on the CTL epitope ^{72}GALPTSVTFELLF^{85} four amino acid replacements were found for the three positively selected strains (Figure 3a). The substitution G72R, described as a mutation caused by positive selective pressure (Perez, Diaz de Arce, et al., 2012a) was present in all three selected strains. In addition, the amino acid change L74S was found in the strains CSFV/Holguin (CSF1056)/2009 and CSFV/Pinar del Rio (CSF1058)/2010, whereas the amino acid changes V78A and T79A were found in the strains CSFV/Holguin (CSF1056)/2009 and CSFV/Santiago de Cuba (CSF1057)/2011, respectively (Figure 3a). Likewise, a replacement in the residue T340A on the CTL epitope ^{331}VTDHHSDYFTEF^{343} was found in all three emergent strains (Figure S2). Thus, alterations on these CTL epitopes could facilitate the escape of these viral strains to the immune response elicited by the vaccine, providing them additional evolutionary advantages.

A total of 12 B-cell epitopes were indistinctively detected by the three methods used (Table S1). From this pool of epitopes, a total of seven overlapping B-cell epitopes were initially selected (Table 2). After a posterior evaluation for antigenicity, one of the selected epitopes was discarded and from the remaining six epitopes, only four candidates that were detected in parallel by TCD4+ method, were finally considered as B-cell epitopes in our analysis (Table 2).

The neutralizing antibody response of the host is mainly elicited against the B-cell epitopes of the E2 viral protein. Although the Erns protein can also induce an antibody response, results have shown that Erns exhibits a weak neutralizing effect towards CSFV (Konig, Lengsfeld, Pauly, Stark, & Thiel, 1995). Therefore, considering the high neutralizing titre of antibodies used in the cross-neutralization approach, we only considered the contribution of the E2 viral protein. To decipher the causes of the antigenic differences found between the viral strains studied, we initially analysed the multiple sequence alignment for E2 protein between the ancestral CSFV strain and the positively selected strains (Figure S2). Thus, two residues substitution located on the B-cell epitope ^{78}VTFELFDGTSPSIEEMGDDFGFGLGLCPF^{107} in the strains CSFV/Holguin (CSF1056)/2009 and CSFV/Santiago de Cuba (CSF1057)/2011 and one substitution in the strain CSFV/Pinar del Rio (CSF1058)/2010 were found (Figure S2 and Figure 3b). Since the CSFV/Pinar del Rio (CSF1058)/2010 strain did not show any significant antigenic difference with the ancestral strain CSFV/Margarita (CSF0705)/1958, we assumed that the substitution I91V found on the B-cell epitope ^{78}VTFELFDGTSPSIEEMGDDFGFGLGLCPF^{107} on the three positively selected strains (Figure 3b) does not contribute to antigenic changes. On the other hand, the substitutions (V78A and T79A, Figure 3b) found in the strains CSFV/Holguin (CSF1056)/2009 and CSFV/Santiago de Cuba (CSF1057)/2011, but not in the CSFV/Pinar del Rio (CSF1058)/2010 strain could produce steric hindrance on B-cell epitope ^{78}VTFE(*LFDGTSPSIEEMGDD*)FGFGLGLCPF^{107} explaining the antigenic differences found in these

TABLE 5 Coefficients of antigenic diversity (1/r) between the ancestral CSFV strain and three emergent CSFV by positive selection pressure

Relation Strain A versus Strain B	1/r*
CSFV/Holguin(CSF1056)/2009 versus CSFV/Margarita(CSF0705)/1958	1.64
CSFV/Pinar del Rio(CSF1058)/2010 versus CSFV/Margarita(CSF0705)/1958	0.77
CSFV/Santiago de Cuba(CSF1057)/2011 versus CSFV/Margarita(CSF0705)/1958	1.65
CSFV/Holguin(CSF1056)/2009 versus CSFV/Pinar del Rio(CSF1058)/2010	**2.00**
CSFV/Holguin(CSF1056)/2009 versus CSFV/Santiago de Cuba(CSF1057)/2011	1.84
CSFV/Pinar del Rio(CSF1058)/2010 versus CSFV/Santiago de Cuba(CSF1057)/2011	**2.00**

*For *r* calculation see equation (1) in material and method. Values represent antigenic distance metric for the CSFV strains estimated using the following equation (1). Antigenic distances resulting 0.5 < (1/r) < 1.5 indicate no significant antigenic difference between the two viruses, results of 1.5 < (1/r) < 2 indicates antigenic difference between the two viruses, whereas (1/r) < 2 means that the two virus strains present major antigenic difference. For more detail see Table S6 and Archetti and Horsfall (1950).
Values of antigenic distance equal or higher than two were denoted in bold.

two strains by cross-neutralization approach compared to the ancestral strain (Table 5).

3.2.3 | Evaluation of amino acid substitution driving deimmunization on E2 protein of CSFV

To corroborate the previous finding, an additional evaluation for deimmunization properties of the E2 protein of CSFV was conducted. A total of 235 amino acid substitutions were detected inducing immunogenicity alterations on seven immunogenic peptides (Table S8). Considering only those substitution found in the strains studied in the current work, we focused our analysis in three immunogenic variations. The amino acid substitution I18K in the CSFV/Santiago de Cuba (CSF1057)/2011 strain yielded a score value = 3 (Table S8 and Figure 3). This value represents a deimmunization of the peptide and the neighbouring peptides. The residue I18 belongs to one of the two TCD4+ epitopes involved in the activation of the neighbouring B-cell epitope ^{24}EGLTTTWKDYDHNLQLDDGTIKA^{47}. Thus, the I18K substitution in the CSFV/Santiago de Cuba (CSF1057)/2011 strain induces a reduction in the antigenicity of B-cell epitope ^{24}EGLTTTWKDYDHNLQLDDGTIKA^{47} (Figure 3c), facilitating the escape of this strain to the antibody response induced by the vaccine and showing an antigenic difference with the ancestral strain CSFV/Margarita (CSF0705)/1958 as evidenced by cross-neutralization analysis. Likewise, the substitutions V78A and T79A on CSFV/Holguin (CSF1056)/2009 and CSFV/Santiago de Cuba (CSF1057)/2011, respectively, yielded score values equal to 3 (Table S8 and Figure 3d,e). These results indicate that both substitutions reduce the antigenicity of peptide ^{72}GALPTSVTFELLF^{85} (one of the immunogenic CTL epitopes; Table 4) and the neighbouring epitope ^{78}VTFE*LFDGTSPSIEEMGDD*FGFGLGLCPF^{107} (one of the immunogenic B-cell epitopes for both emergent strains; Table 2; Figure 3c,d).

On the one hand, the substitutions V78A and T79A on CSFV/Holguin (CSF1056)/2009 and CSFV/Santiago de Cuba (CSF1057)/2011, respectively, affect the recognition and immunogenicity of the CTL epitope ^{72}GALPTSVTFELLF^{85} (Figure 3d,e). These mutations could facilitate the escape to the adaptive cellular immune response of the host (naturally or vaccine induced) without reflecting any changes on the antigenicity results. On the other hand, since substitutions V78A and T79A on CSFV/Holguin (CSF1056)/2009 and CSFV/Santiago de Cuba (CSF1057)/2011, respectively, also decrease the immunogenicity of the B-cell epitope ^{78}VTFE*LFDGTSPSIEEMGDD*FGFGLGLCPF^{107} (Figure 3d,e), which is reflected as an escaping to the antibody immune response (humoral response), these mutations could impair the adaptive humoral response of the host (naturally or vaccine induced) to neutralize these viral strains, generating a change in the antigenicity compared to the ancestral strain CSFV/Margarita (CSF0705)/1958 and the positively selected strain CSFV/Pinar del Rio (CSF1058)/2010.

Thus, taking together the results, the deimmunization approach strongly suggests that the residue replacements V78A on CSFV/Holguin (CSF1056)/2009 and on T79A CSFV/Santiago de Cuba (CSF1057)/2011, cause a decrease in the recognition by the antibody response and are responsible for changes in antigenicity in CSFV, which was confirmed by cross-neutralization test.

3.3 | Spatiotemporal analysis and clinical signs comparison between high- and low-rate clusters

Precision surveillance applies spatiotemporal analytics to routinely collected surveillance data to identify loci with increased risk of disease (Cummings et al., 2019). Thus, surveillance approaches from large and small spatial scales play an essential role in health decision-making and the scientific investigation of infectious diseases. However, such data are subject to missing observations, delays in reporting, and observational biases that can lead to increased uncertainty and incorrect conclusions (Lee et al., 2018). Considering these factors, the information used in the current study was detailed and spatially segregated by 1 km^2 quadrants. Thus, the spatiotemporal analysis and the characterization of rate clusters were refined to gain in reliability and accuracy. Considering the information obtained from National Laboratory for Veterinary Diagnostic (NLVD), during 2010–2016 a total of 846 foci were reported in Cuba. Using the information reported by affected

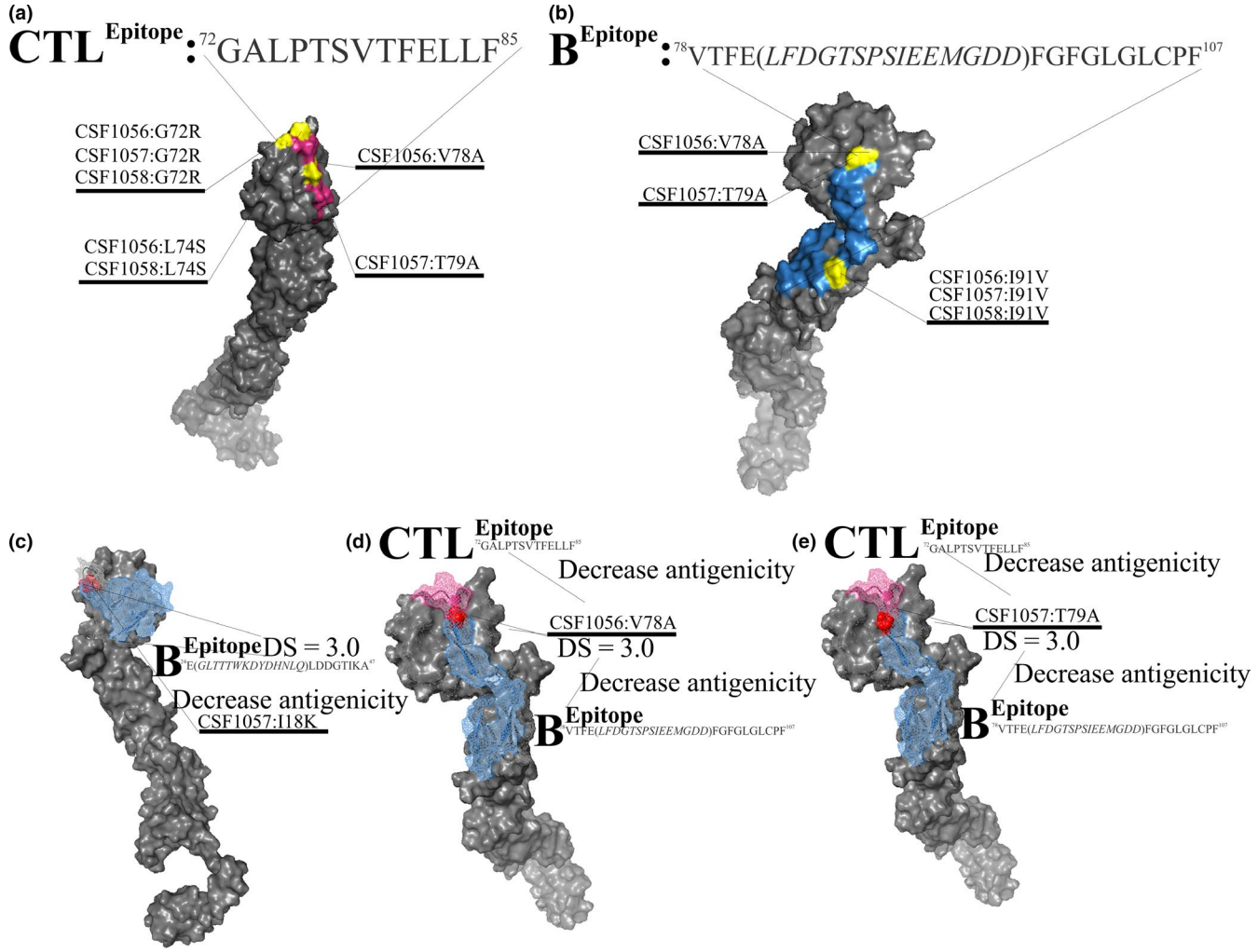

FIGURE 3 Three-dimensional representation of mutations on E2 model located on CTL, B-cell epitopes and deimmunization sites. In all the cases, the E2 model solid surface is presented in gray, the CSFV/Santiago de Cuba (CSF1057)/2011 was denoted as CSF1057, the CSFV/Holguin (CSF1056)/2009 strain was denoted as CSF1056, and the CSFV/Pinar del Rio (CSF1058)/2010 strain was denoted as CSF1058. (a) Representation of the amino acid replacements on CTL-epitope of the E2 protein for the three positively selected strains in comparison with the ancestral strain CSFV/Margarita (CSF0705)/1958, the CTL epitope 72GALPTSVTFELLF85 is denoted in pink, all the mutations presented in positively selected strains on this CTL epitope are denoted in yellow, the amino acid replacement presented in each strain is also denoted. (b) Representation of the amino acid replacements on B-cell epitope of the E2 protein for the three positively selected strains in comparison with the ancestral strain CSFV/Margarita (CSF0705)/1958, the B-cell epitope 78VTFELFDGTSPSIEEMGDDFGFGLGLCPF107 is denoted in blue, all the mutations presented in positively selected strains on this B-cell epitope are denoted in yellow, the amino acid replacement presented in each strain is also denoted. (c) Evaluation of deimmunization induced by amino acid replacement I18K presented in E2 protein of CSFV/Santiago de Cuba (CSF1057)/2011 (denoted by red spheres), the score of deimmunization is also denoted (DS), the effect of deimmunization on B-cell epitope 78VTFELFDGTSPSIEEMGDDFGFGLGLCPF107 (blue) is also denoted. (d) Evaluation of deimmunization induced by amino acid replacement V78A presented in E2 protein of CSFV/Holguin (CSF1056)/2009 (denoted by red spheres), the score of deimmunization is also denoted (DS), the effects of deimmunization on the B-cell epitope 78VTFELFDGTSPSIEEMGDDFGFGLGLCPF107 (blue) and the CTL epitope 72GALPTSVTFELLF85 (pink) are also denoted. (e) Evaluation of deimmunization induced by amino acid replacement T79A presented in E2 protein of CSFV/Santiago de Cuba (CSF1057)/2011 (denoted by red spheres), the score of deimmunization is also denoted (DS), the effects of deimmunization on the B-cell epitope 78VTFELFDGTSPSIEEMGDDFGFGLGLCPF107 (blue) and the CTL epitope 72GALPTSVTFELLF85 (pink) are also denoted. (The list of all deimmunization sites found in the study and the deimmunization score are listed in Table S8) [Colour figure can be viewed at wileyonlinelibrary.com]

premises during this same period and through the space-time permutation, a total of four high-rate clusters (H1, H2, H3 and H4) were detected (Figure 4). The values obtained determined that in the areas where the high-rate clusters were detected, holdings were H1 = 4.48-fold (period = 2011), H2 = 3.29-fold (period = 2014), H3 = 4.33-fold (period = 2010) and H4 = 2.06-fold (period = 2012) more CSF-affected than the expected for each period during 2010–2016 (Table 6). On the other hand, two low-rate clusters were identified (Figure 4). In the geographical areas where these low clusters were located, the number of CSF-affected pig holdings was consequently lower (L1: relative risk

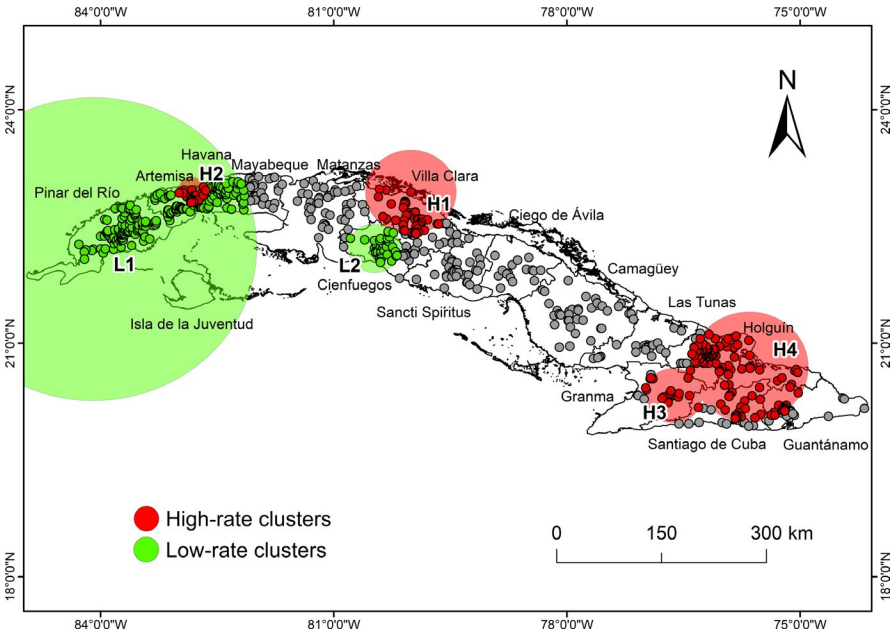

FIGURE 4 Spatiotemporal distribution of predicted high- and low-rate clusters of CSF-affected pig holdings in Cuba during 2010–2016. Low-rate clusters of CSF-affected pig holdings (L1 and L2) (denoted in green) and high-rate clusters of CSF-affected pig holdings (H1-H4) (denoted in red) are shown. All affected holdings are represented by dots. Grey dots are holdings outside clusters. Red and green dots are holdings from high- and low-rate clusters, respectively. The area of the clusters is indicated. All the regional location of Republic of Cuba are also denoted [Colour figure can be viewed at wileyonlinelibrary.com]

TABLE 6 Features of high- and low-rate spatiotemporal clusters of CSF-affected pig holdings in Cuba during 2010–2016

	High-rate clusters				Low-rate clusters	
Cluster	**H1**	**H2**	**H3**	**H4**	**L1**	**L2**
Latitude	22.94331	22.96928	20.32697	20.69341	22.20936	22.22004
Longitude	−80.00863	−82.82360	−76.63223	−75.65264	−84.09414	−80.47622
Radius (km)	59.99	18.09	39.06	78.99	216.34	34.89
Start year	2011	2014	2010	2012	2010	2012
End year	2011	2014	2010	2012	2012	2013
Locations	45	21	18	112	229	38
p-value	0.000004	0.007635	0.016	0.033	0.000409	0.0088
Observed	20	18	12	36	51	0
Expected	4.46	5.48	2.77	17.45	95.01	10.78
ODE	4.48	3.29	4.33	2.06	0.54	0.00

[RR] = 0.58 and L2: RR = 0) than expected in the period 2010–2012 and 2012–2013, respectively (Table 6).

From the total of 11 clinical signs assessed, only the presentation of respiratory clinical manifestation showed significant differences when CSF-affected pig holding from high-rate clusters and low-rate clusters were compared (Table 7). Thus, these results clearly indicated that the respiratory clinical manifestations were less frequently present (OR = 0.44, 0.216–0.898) in pig holdings from high-rate clusters than in low-rate clusters.

4 | DISCUSSION

Despite the implemented efforts by many government authorities to control and eradicate CSF from national pig populations, the disease remains as a significant challenge for the scientific community and the animal health (Xie et al., 2018). The current re-emergence of CSF in several countries including Brazil (https://www.oie.int/wahis_2/public/wahid.php/Reviewreport/Review?page_refer=MapFullEventReport&reportxml:id=28416), Japan (http://www.oie.int/wahis_2/temp/reports/en_imm_0000027871_20180910_161441.pdf), Ecuador (Garrido Haro, Barrera Valle, Acosta, & Flores, 2018) and South Korea (Je et al., 2018) clearly shows the major concern that represents a possible global re-emergence of this disease (Xie et al., 2018). This situation deserves especial attention, considering that the countries that have reported new outbreaks of CSF have also reported the emergence of new strains, such as subgenotype 1.6 in Brazil (Silva et al., 2017), subgenotype 1.7 in Ecuador (Rios, Nunez, Diaz de Arce, Ganges, & Perez, 2018) or the reversion to the virulence of the vaccine strain LOM in Korea (Je et al., 2018). Therefore, in the current situation, the scientific community is facing two big challenges regarding CSF. On the one hand, since the

TABLE 7 Comparison of reported clinical signs between high- and low-rate clusters from CSF-affected pig holdings

Variable		Cluster		*p*-value	OR	95% CI	
		H	L			Lower	Upper
Loss of appetite	Yes	53	29	.582	1.218	0.602	2.464
	No	33	22				
Fever	Yes	78	48	.480	0.609	0.154	2.410
	No	8	3				
Conjunctivitis	Yes	50	35	.223	0.635	0.306	1.318
	No	36	16				
Diarrhoea	Yes	48	32	.427	0.750	0.369	1.525
	No	38	19				
Lack of coordination	Yes	25	18	.448	0.751	0.359	1.574
	No	61	33				
Cyanosis/Petechial haemorrhages	Yes	35	26	.243	0.660	0.329	1.325
	No	51	25				
Neurological signs	Yes	35	20	.864	1.064	0.524	2.159
	No	51	31				
Respiratory signs	Yes	27	26	.024*	0.440	0.216	0.898
	No	59	25				
Poor growth	Yes	17	8	.551	1.324	0.526	3.332
	No	69	43				
Abortions and stillbirths	Yes	2	1	.888	1.190	0.105	13.466
	No	84	50				
Mummification and malformations	Yes	0	1	1.000	–	–	–
	No	86	50				
Total	86	51					

Note: Abbreviations: CI, confidence interval; H, high-rate cluster; L, low-rate cluster; OR, odds ratio.
*Statistical differences ($p < .05$)

molecular mechanisms driving the evolution, antigenic diversity, virulence and pathogenesis of CSFV are still poorly understood (Rios et al., 2018; Wang et al., 2018), the implementation of control programs to prevent outbreaks of new emergent strains is far from being achieved. On the other hand, if it is considered that the vaccination programs for the control of CSF are mainly based on live modified vaccines or lapinized vaccines developed during the mid-1950s, together with the issue that the parameter to consider full protection against CSFV in most countries, is based on the capacity of these vaccines to induce certain titres of neutralizing antibodies (Xing et al., 2018), then, in-depth researches are urgently needed to explain the mechanisms by which CSFV evades the cell-mediated immune response, which compromise the efficacy of these vaccines. Furthermore, the reinspection of the parameters to evaluate the vaccines in use (protective doses, efficacy against different emerged strains induced by the action of positive selection pressure and interaction with immunosuppressant viral agents such as PRRS and PCV2) is also imperative investigations to conduct.

The current study provides a comprehensive picture about the pathogenesis, virulence, and antigenicity of new emergent CSFV strains resulting from the action of the positive selection pressure. The effect of the circulation of these strains on surveillance systems in an endemic region to CSF was also assessed. Positively selected strains have mainly emerged as result of the implementation of failed vaccination programs (Hu et al., 2016; Ji et al., 2014; Perez, Diaz de Arce, et al., 2012a), indicating that the application of improper evaluated vaccines (unable to induce complete sterile immunity under field conditions) could carry, in the long-term, harmful and unpredicted consequences for the global emergence and potential spreading of CSFV. Despite several reports suggesting that the emergence of positively selected strains leads to changes in the genetic structure of the viral population (Hu et al., 2016; Ji et al., 2014; Perez, Diaz de Arce, et al., 2012a), the effect of this evolutionary force on viral virulence and pathogenesis remains unclear.

In this regard, a recent report by Wang et al. (2018) attempted to assess the pathogenesis of the current emergent strains of CSFV in China (Wang et al., 2018). However, the mentioned study presented a serious limitation, since it only included one of the current emergent CSFV strains (Wang et al., 2018), which had been previously classified by Luo et al. (2017) as moderately virulent, showing also antigenic differences with the historically Chinese strain Shimen (Luo et al., 2017). In the current work, to avoid any possible bias in the

evaluation of virulence and pathogenesis of new positively selected strains and to obtain broader information, three different strains isolated from different years and located geographically distant (Perez, Diaz de Arce, et al., 2012a) were included. The results obtained showed clear differences in the virulence degree of the strains assessed. The strain CSFV/Santiago de Cuba (CSF1057)/2011 resulted in a highly virulent strain resembling its ancestral strain CSFV/Margarita (CSF0705)/1958. It is important to denote that CSFV/Margarita (CSF0705)/1958 strain caused the origin of the Cuban epidemic outbreaks in 1993 as a consequence of a viral escape to the field (Díaz de Arce et al., 1999) which has lasted until the current days. However, the remaining two strains showed a decrease in virulence. Thus, the strain CSFV/Holguin (CSF1056)/2009 showing a pattern of a moderate degree in virulence and the CSFV/Pinar del Rio (CSF1058)/2010 consistent with the previous characterization described in Postel et al. (2015) showed a pattern of low virulence. Considering that the selective pressure takes place on immunogenic structural viral proteins, for CSFV most of these sites has been identified on E2 (Hu et al., 2016; Perez, Diaz de Arce, et al., 2012a; Tang, Pan, & Zhang, 2008), affecting the viral attachment, tropism and viral load into the host. Then, the decrease in virulence in CSFV/Holguin (CSF1056)/2009 and CSFV/Pinar del Rio (CSF1058)/2010 seems to be a direct consequence of the action of the bottleneck effect followed by the selection of the escaping variants. However, the unexpected pattern is shown by the strain CSFV/Santiago de Cuba (CSF1057)/2011 resulting in the same virulence degree of the parental strain CSFV/Margarita (CSF0705)/1958 could be related with additional complex aspects. We hypothesized that two main factors could lead to the highly virulent pattern shown for this strain. First, it is important to highlight the fact that CSFV is a quasispecies virus, hence the viral population consists of a mutant spectrum (Domingo, Sheldon, & Perales, 2012). The mutant spectra are a source of virus adaptability since they constitute dynamic repositories of genotypic and phenotypic viral variants (Domingo et al., 2012). Therefore, whereas the bottleneck effect introduces in the viral population a strong element of stochasticity during the selection process, mainly at the short-term (intrahost), later with different viral passages (interhost), the viral population tends to re-gain the viral fitness, mainly triggered by the environment (Escarmis, Davila, & Domingo, 1999). The fitness gain is the result of competitive optimization of a viral quasispecies in its tendency towards a mutation-selection equilibrium in a given environment (Escarmis et al., 1999). It has been previously documented that in Cuba, a strict geographical segregation has been established to control the movement of swine populations among the different regions (Perez, Arce, Cortey, et al., 2011a). Thus, since the CSFV/Santiago de Cuba (CSF1057)/2011 strain is the most recently collected field strain compared to the other strains in this study, it is highly probable that the viral evolution for this strain, in a segregated microenvironment, has facilitated the re-gain of the viral fitness, resulting in broader mutant spectra for its viral quasispecies. Indeed, studies of microevolution have shown that virus particle may not be capable of initiating an infection and producing progeny at a given time, but the same particle may immediately be exposed to a different environment that triggers its replication by the gain of viral fitness of its quasispecies cloud (Domingo et al., 2012). Moreover, the high diversity in viral quasispecies in CSFV (broader mutant spectra) has been directly linked to high virulence pattern (Topfer et al., 2013). Therefore, the gaining in fitness by the CSFV/Santiago de Cuba (CSF1057)/2011 strain, could clearly be the consequence of the enhanced virulence of this strain. A second factor to consider is that proteins other than E2 have been also linked to enhance the virulence of CSFV, such as Npro (Tamura et al., 2014) and NS4B (Leifer, Ruggli, & Blome, 2013; Tamura et al., 2012). Thus, while the positive selection pressure on E2 protein of CSFV seems to induce a decrease in virulence, it is possible that the compensation action of other markers of virulence into the quasispecies cloud could be enough to yield a highly virulent phenotype. Nonetheless, to confirm both hypotheses, further studies based on deep sequencing analysis would be required.

The pathogenicity results from the studied strains matched the virulence degree determined for each strain based on the clinical score. Thus, the viral load in all the tissues assessed, duration of viremia and viral shedding for the strains CSFV/Santiago de Cuba (CSF1057)/2011 and the parental strain CSFV/Margarita (CSF0705)/1958 were statistically higher than for the strains CSFV/Holguin (CSF1056)/2009 and CSFV/Pinar del Rio (CSF1058)/2010. Similar results were obtained by Weesendorp et al. (2009) when the dynamics of viral infection and excretion during the entire infectious period were compared among highly, moderately or low virulent CSFV strains (Weesendorp et al., 2009). Likewise, considering the results obtained in this study in comparison with the finding previously described by Weesendorp et al. (2009), it seems to be a characteristic of the low and moderate virulent CSFV strains to be restricted to a nasal (oropharyngeal) transmission. This finding also concours with the clinical observations in field about the outbreaks caused by the current emergent CSFV strains reporting as main clinical signs, respiratory disorders (Luo et al., 2017; Perez, Diaz de Arce, et al., 2012a). Based on the results obtained here, it is important to highlight the risk represented by the circulation of low virulent strains of CSFV in endemic areas, since the animals infected do not present any clinical signs indicating CSFV infection but can shed high viral loads during long periods of time, facilitating the viral circulation in the field.

The E2 protein of CSFV plays a relevant role in inducing immune protection against the viral infection and it is, therefore, prone to immune pressure to generate antigenic variation more easily (Hu et al., 2016; Perez, Diaz de Arce, et al., 2012a; Rios et al., 2017; Shen et al., 2011; Tang et al., 2008). The combination of epitope and deimmunization classification, with antigenic characterization by cross-neutralization and antigenic metric distance estimation, enables the development of antigenic maps for viral agents such as influenza virus (Li et al., 2013; Liu et al., 2015; Peng et al., 2017) or Newcastle disease virus (Liu et al., 2017). Indeed, this methodology has been successfully applied to establish early control measures for certain emergent strains of these viral agents, including changes to the type

of vaccines to be used (Li et al., 2013; Liu et al., 2017). To our knowledge, this is the first report applying the use of immunoinformatic approaches to characterize both T-cell and B-cell epitopes for the main immunogenic protein of CSFV (E2 protein), combining also cross-neutralization and antigenic metric distance estimation for this viral agent. The results obtained allow us to infer in the first place that CSFV strains can antigenically evolve (changes in antigenicity) without undergoing subgenotype changes, since all the strains used in the study of the antigenic evaluation belonged to the subgenotype 1.4 (Rios et al., 2018). Likewise, a better understanding regarding the role of the positive selection pressure on antigenic changes, immune system escaping or additional properties of CSFV can be achieved. First, examining all the positively selected sites described in the literature, Tang et al. (2008) reported the sites 72, 75 and 200; Shen et al. (2011) found the sites 49 and 72; Perez, Diaz de Arce, et al. (2012a) described the sites on B/C domain 34, 36, 49, 72, 87 and 88; Hu et al.(2016) reported the sites 34, 72, 168, 200, 240 and 283, and Rios et al. (2017) found the sites 20, 49, 72, 200, and 268. Combining these results described in the literature with the characterization obtained in the current study, we can easily infer that, the selected site of the E2 protein at position 72 seems to be critical to escape the immune response of the host, especially considering that this site is located on a CTL epitope and it is reported by all the research groups regardless of the CSFV genotype, year of collection of the strains or geographical location. Therefore, the CTL epitope ^{72}(GALPTSVTF)ELLF^{85}, reported here, merits an especial attention for the future development of new strategic vaccines. Regarding the other reported sites under positive selection, we can also define that, position 34 commonly described by Perez, Diaz de Arce, et al. (2012a) and Hu et al. (2016), as well as the position 75 described by Tang et al.(2008), is also located on CTL epitopes and can facilitate the escape of CSFV to the immune response of the host elicited by the vaccines without evidences of antigenic changes in the E2 protein of the CSFV strains. On the other, the sites at position 87, 88 (Perez, Diaz de Arce, et al., 2012a), 200 (Hu et al., 2016; Rios et al., 2017; Tang et al., 2008), and 283 (Hu et al., 2016) can be located on B-cell epitopes. Thus, variation on these sites can decrease the immune efficacy of the vaccines in use, favouring also antigenic changes on E2 protein. On deimmunization sites, the only positively selected site found was the position 20 described by Rios et al. (2017), hence, variation on this position can induce decrease in the immunogenicity for the B-cell epitope ^{24}E(*GLTTTWKDYDHNLQ*)LDDGTIKA^{47} and the CTL epitope ^{26}LTTTWKDY^{34}. However, other positively selected sites such as the positions 17 (Hu et al., 2016), 49 (Perez, Diaz de Arce, et al., 2012a; Rios et al., 2017; Shen et al., 2011), 168, 283 (Hu et al., 2016) and 268 (Rios et al., 2017) were not found located on any CTL or B-cell epitopes. Therefore, these sites are probable linked to additional properties of the virus including changes in tropism, virus attachment, viral entry or others. However, experiments using reverse genetic approaches will be required to confirm this last hypothesis. Likewise, molecular dynamic approach combined with docking analyses to uncover folding stability of E2 in its homodimer or heterodimer formation (E2E1) will be also needed. The cross-neutralization assay used in the current study allows to identify additional mutations other than positively selected sites linked to changes in antigenicity. However, to expand this result to other strains circulating in other geographical areas, cross-neutralization results from different strains are required. Whereas Reference Laboratories for Avian influenza virus are focused on assessing and storing data related to virus neutralization from different strains measured by inhibition of hemagglutination (Ren et al., 2015), which facilitates the antigenic map reconstructions, this kind of information is unfortunately unavailable for CSFV. Therefore, the creation of a Reference Database containing virus cross-neutralization results from different strains of CSFV facilitating the evaluation of the antigenic evolution for this viral agent will be a valuable aim to accomplish.

Interrupting transmission by the early recognition of cases and the identification of high-risk populations has been recognized as a critical step to stop outbreaks of infectious diseases (Cummings et al., 2019). In this regard, spatiotemporal statistical approaches have become valuable tools, adding precision to qualitative verbal descriptions, facilitating the comparison of distributions, drawing attention to characteristics unlikely to be noticed by visual inspection and understanding how disease phenomena behave (Ward, 2007). Combining the information obtained from the analysis of virulence and pathogenicity of the emergent CSFV strains assessed with the spatiotemporal distribution of CSF-affected holdings, a direct relationship was found. Thus, in Pinar del Rio province where the low virulent strain was initially isolated (Perez, Diaz de Arce, et al., 2012a) a low-rate spatiotemporal cluster (L1) was identified, whereas the two biggest high-rate spatiotemporal clusters (H3 and H4) where located in the eastern region of the country, including the provinces where the highly virulent strain and the moderately virulent strain were isolated (Perez, Diaz de Arce, et al., 2012a). The presence of low virulent strains of CSFV has been considered as a source of virus dissemination very difficult to detect, mainly because the clinical signs are almost absent and infected pigs are hard to recognize (Weesendorp et al., 2009). Indeed, clinical manifestations of respiratory diseases have been mainly observed in those herds where positively selected strains have been identified (Luo et al., 2017; Perez, Diaz de Arce, et al., 2012a). Therefore, the presence of a low-rate spatiotemporal cluster could be an indicator of low sensibility of the disease surveillance system to detect the circulation of this kind of strains. This issue is a key factor that could be contributing to the under-report of the disease, enabling the perpetuity of CSFV in the field and favouring the endemism of the disease, resulting in a challenge for the current system of epidemiological surveillance. Conversely, the infections caused by highly virulent strains result in large amounts of virus excreted, and the infected pigs are relatively easy to recognize since the clinical signs are compatible with CSF (Weesendorp et al., 2009). Then, it is expected that in regions where highly virulent strains are circulating, an increase in the reports of CSF takes place, contributing this way to the presence of high-rate spatiotemporal clusters. Interestingly, this study found both the high-rate (H1) and a low-rate (L2) clusters in the central region of the country. This unexpected pattern could be a consequence of the organization of the Cuban swine

genetic replacement, which is conducted in the central region of the country (Perez, Arce, Cortey, et al., 2011a). In this particular region of Cuba, the crossing of three main swine breeds take place: the reproductive sows *Landrace* breed and *Large White* breed are collected from the western region of the country whereas the *Duroc* breed reproductive boars are collected from the eastern region of the country (Perez, Arce, Cortey, et al., 2011a; Rios et al., 2018). After the genetic crossing, the resulting animals are segregated geographically. Thus, the point of concentration for the animal genetic crossing results in a mixing vessel for the strains from both sides of the country; hence, clinical manifestations compatible with the acute and subclinical forms of CSF can be observed, resulting in an additional challenge for the epidemiological surveillance system established in Cuba. Indeed, since strains from both sides of the country can be mixed during the event of animal genetic crossing, this issue could have potentially led to the occurrence of a high-rate cluster H2 in 2014 in the western half of the country, after the previously identified low-rate cluster L1 in this same region, suggesting the co-circulation of both low- and highly virulent strains in the same region. However, the impact on the *quasispecies* composition for the viral population circulating, and immune response of the affected animal in the farms affected with this kind of infection (mixed infections) is completely unknown, requiring further studies for a better understanding.

5 | CONCLUSION

The current study provides novel and significant insights into variations in virulence, pathogenesis and antigenicity experienced by CSFV strains after positive selection pressure effect. The results obtained suggest that the action of the positive selection pressure induces a decrease in virulence, with alterations in pathogenicity and antigenicity. However, the evolutionary process of CSFV, especially in segregated microenvironments, could contribute to the fitness-gain event, restoring the highly virulent pattern of the circulating strains. Besides, we denoted that the presence of low virulent strains selected by bottleneck effect after inefficient vaccination can lead to a relevant challenge for the epidemiological surveillance of CSF, contributing to the under-reports of the disease and favouring the perpetuation of the virus in the field. In this study, B-cell and CTL epitopes on the E2 3D-structure model were also identified, this approach combined with the cross-neutralizing technic allows to define antigenic variants for CSFV, which represent a critical step for the development of novel and more efficient vaccines such as multi-epitope vaccines. Nevertheless, to extent this last finding to other geographical regions affected by CSFV, the creation of cross-neutralization databases, which could facilitate the estimation of antigenic maps for CSFV, are an imperative requirement.

ACKNOWLEDGEMENTS

The authors would also like to thank to D.M.V. Sara Castell from CENSA, for the technical assistance provided during the in vitro experiments and D.M.V Gerardo Hernandez Gonzalez for his outstanding animal care.

CONFLICT OF INTEREST

The authors declare no conflict of interest.

AUTHOR CONTRIBUTIONS

L.J.P. and O.F. designed the research; L.C. and FP performed the pathogenesis and virulence analyses; L.R performed the immunoinformatic approaches; L.C, L.R, P.N. and C.L.P contributed to the antigenic evaluations; L.A., M.T.F. and M.I.P. contributed to the epidemiological studies. L.C., L.R., C.L.P., O.F. and L.J.P. analysed and interpreted the data; L.C. and L.J.P. wrote the paper; L.R., O.F. and L.J.P. edit the paper and provided intellectual inputs. All the authors read and approved the final version of the manuscript.

ETHICAL APPROVAL

International standards for animal welfare were used for all animal samples collected, following the regulations of the Animal Health Department (AHD), Ministry of Agriculture (MINAGRI) of the Republic of Cuba. The protocol # PNO-G-040-2016 of the National Center for Animal and Plant Health (CENSA) was approved by the Committee on the Ethics of the MINAGRI of the Republic of Cuba and all efforts were made to minimize the suffering of the animals. Since the AHD is the official regulatory body of the Republic of Cuba, additional permits were not required.

GUARANTOR STATEMENT

Dr. Lester J. Pérez and Dr. Osvaldo Fonseca are the guarantors of this work, had full access to all the data, and take full responsibility for the integrity of data and the accuracy of data analysis.

ORCID

Liliam Rios http://orcid.org/0000-0002-2763-5431
Osvaldo Fonseca-Rodriguez https://orcid.org/0000-0002-0253-5928
Lester J. Perez https://orcid.org/0000-0002-5717-5181

REFERENCES

Ali, M., Pandey, R. K., Khatoon, N., Narula, A., Mishra, A., & Prajapati, V. K. (2017). Exploring dengue genome to construct a multi-epitope based subunit vaccine by utilizing immunoinformatics approach to battle against dengue infection. *Scientific Reports*, *7*, 9232.
Andreatta, M., & Nielsen, M. (2016). Gapped sequence alignment using artificial neural networks: Application to the MHC class I system. *Bioinformatics*, *32*, 511–517.
Archetti, I., & Horsfall, F. L. Jr (1950). Persistent antigenic variation of influenza A viruses after incomplete neutralization in ovo with

heterologous immune serum. *The Journal of Experimental Medicine*, *92*, 441–462.

Ashraf, N. M., Bilal, M., Mahmood, M. S., Hussain, A., & Mehboob, M. Z. (2016). In-silico analysis of putative HCV epitopes against Pakistani human leukocyte antigen background: An approach towards development of future vaccines for Pakistani population. *Infection, Genetics and Evolution : Journal of Molecular Epidemiology and Evolutionary Genetics in Infectious Diseases*, *43*, 58–66.

Backert, L., & Kohlbacher, O. (2015). Immunoinformatics and epitope prediction in the age of genomic medicine. *Genome Medicine*, *7*, 119.

Blome, S., Moss, C., Reimann, I., Konig, P., & Beer, M. (2017a). Classical swine fever vaccines-State-of-the-art. *Veterinary Microbiology*, *206*, 10–20.

Blome, S., Staubach, C., Henke, J., Carlson, J., & Beer, M. (2017b). Classical swine fever-an updated review, *Viruses*, *9*, E86.

Chen, J., Liu, H., Yang, J., & Chou, K. C. (2007). Prediction of linear B-cell epitopes using amino acid pair antigenicity scale. *Amino Acids*, *33*, 423–428.

Coronado, L., Liniger, M., Munoz-Gonzalez, S., Postel, A., Perez, L. J., Perez-Simo, M., … Ganges, L. (2017). Novel poly-uridine insertion in the 3'UTR and E2 amino acid substitutions in a low virulent classical swine fever virus. *Veterinary Microbiology*, *201*, 103–112.

Cummings, M. J., Tokarz, R., Bakamutumaho, B., Kayiwa, J., Byaruhanga, T., Owor, N., …, O'Donnell, M. R. (2019). Precision surveillance for viral respiratory pathogens: virome capture sequencing for the detection and genomic characterization of severe acute respiratory infection in Uganda. *Clinical Infectious Diseases: an Official Publication of the Infectious Diseases Society of America*, *68*, 1118–1125.

de Arce, H. D., Ganges, L., Barrera, M., Naranjo, D., Sobrino, F., Frias, M. T., & Nunez, J. I. (2005). Origin and evolution of viruses causing classical swine fever in Cuba. *Virus Research*, *112*, 123–131.

Dhanda, S. K., Grifoni, A., Pham, J., Vaughan, K., Sidney, J., Peters, B., & Sette, A. (2018). Development of a strategy and computational application to select candidate protein analogues with reduced HLA binding and immunogenicity. *Immunology*, *153*, 118–132.

Diaz de Arce, H., Nunez, J. I., Ganges, L., Barreras, M., Teresa Frias, M., & Sobrino, F. (1999). Molecular epidemiology of classical swine fever in Cuba. *Virus Research*, *64*, 61–67.

Díaz de Arce, H., Núñez, J. I., Ganges, L., Barreras, M., Teresa Frías, M.,… F. (1999). Molecular epidemiology of classical swine fever in Cuba. *Virus Research*, *64*, 61–67.

Diaz de Arce, H., Perez, L. J., Frias, M. T., Rosell, R., Tarradas, J., Nunez, J. I., & Ganges, L. (2009). A multiplex RT-PCR assay for the rapid and differential diagnosis of classical swine fever and other pestivirus infections. *Veterinary Microbiology*, *139*, 245–252.

Dikhit, M. R., Ansari, M. Y., Vijaymahantesh, K., Mansuri, R., Sahoo, B. R., Dehury, B., … Das, P. (2016). Computational prediction and analysis of potential antigenic CTL epitopes in Zika virus: A first step towards vaccine development. *Infection, Genetics and Evolution: Journal of Molecular Epidemiology and Evolutionary Genetics in Infectious Diseases*, *45*, 187–197.

Dikhit, M. R., Kumar, S., Vijaymahantesh, B. R., Sahoo, R., Mansuri, A., Amit, M. Y., … Das, P. (2015). Computational elucidation of potential antigenic CTL epitopes in Ebola virus. *Infection, Genetics and Evolution: Journal of Molecular Epidemiology and Evolutionary Genetics in Infectious Diseases*, *36*, 369–375.

Dolz, R., Pujols, J., Ordonez, G., Porta, R., & Majo, N. (2008). Molecular epidemiology and evolution of avian infectious bronchitis virus in Spain over a fourteen-year period. *Virology*, *374*, 50–59.

Domingo, E., Sheldon, J., & Perales, C. (2012). Viral quasispecies evolution. *Microbiology and Molecular Biology Reviews: MMBR*, *76*, 159–216.

Doytchinova, I. A., & Flower, D. R. (2007). VaxiJen: A server for prediction of protective antigens, tumour antigens and subunit vaccines. *BMC Bioinformatics*, *8*, 4.

Edwards, S., Fukusho, A., Lefevre, P. C., Lipowski, A., Pejsak, Z., Roehe, P., & Westergaard, J. (2000). Classical swine fever: The global situation. *Veterinary Microbiology*, *73*, 103–119.

El-Manzalawy, Y., Dobbs, D., & Honavar, V. (2008a). Predicting flexible length linear B-cell epitopes. *Computational systems bioinformatics. Computational Systems Bioinformatics Conference*, *7*, 121–132.

El-Manzalawy, Y., Dobbs, D., & Honavar, V. (2008b). Predicting linear B-cell epitopes using string kernels. *Journal of Molecular Recognition: JMR*, *21*, 243–255.

Escarmis, C., Davila, M., & Domingo, E. (1999). Multiple molecular pathways for fitness recovery of an RNA virus debilitated by operation of Muller's ratchet. *Journal of Molecular Biology*, *285*, 495–505.

ESRI. (2009). *ArcGIS 9.3.1*. Redlands, CA: Environmental Systems Research Institute.

Gao, C., He, X., Quan, J., Jiang, Q., Lin, H., Chen, H., & Qu, L. (2017). Specificity characterization of SLA Class I molecules binding to swine-origin viral cytotoxic T lymphocyte epitope peptides in vitro. *Frontiers in Microbiology*, *8*, 2524.

Garrido Haro, A. D., Barrera Valle, M., Acosta, A., & Flores, J. (2018). Phylodynamics of classical swine fever virus with emphasis on Ecuadorian strains. *Transboundary and Emerging Diseases*, *65*, 782–790.

Hu, D., Lv, L., Gu, J., Chen, T., Xiao, Y., & Liu, S. (2016). Genetic diversity and positive selection analysis of classical swine fever virus envelope protein gene E2 in East China under C-strain vaccination. *Frontiers in Microbiology*, *7*, 85.

Je, S. H., Kwon, T., Yoo, S. J., Lee, D. U., Lee, S., Richt, J. A., & Lyoo, Y. S. (2018). Classical swine fever outbreak after modified live LOM strain vaccination in naive pigs, South Korea. *Emerging Infectious Diseases*, *24*, 798–800.

Ji, W., Niu, D. D., Si, H. L., Ding, N. Z., & He, C. Q. (2014). Vaccination influences the evolution of classical swine fever virus. *Infection, Genetics and Evolution: Journal of Molecular Epidemiology and Evolutionary Genetics in Infectious Diseases*, *25*, 69–77.

Kinjo, T., & Yanagawa, R. (1968). Antigenic relationship among strains of infectious canine hepatitis virus. *The Japanese Journal of Veterinary Research*, *16*, 128–136.

Konig, M., Lengsfeld, T., Pauly, T., Stark, R., & Thiel, H. J. (1995). Classical swine fever virus: Independent induction of protective immunity by two structural glycoproteins. *Journal of Virology*, *69*, 6479–6486.

Kulldorff, M. (2014). *SatScan v9.3: Software for the spatial and space-time scan statistics*. Silver Spring, MD: Information Management Services Inc.

Lee, E. C., Arab, A., Goldlust, S. M., Viboud, C., Grenfell, B. T., & Bansal, S. (2018). Deploying digital health data to optimize influenza surveillance at national and local scales. *PLoS Computational Biology*, *14*, e1006020.

Leifer, I., Ruggli, N., & Blome, S. (2013). Approaches to define the viral genetic basis of classical swine fever virus virulence. *Virology*, *438*, 51–55.

Li, Y., Bostick, D. L., Sullivan, C. B., Myers, J. L., Griesemer, S. B., Stgeorge, K., … Hensley, S. E. (2013). Single hemagglutinin mutations that alter both antigenicity and receptor binding avidity influence influenza virus antigenic clustering. *Journal of Virology*, *87*, 9904–9910.

Liu, J., Zhu, J., Xu, H., Li, J., Hu, Z., Hu, S., … Liu, X. (2017). Effects of the HN antigenic difference between the vaccine strain and the challenge strain of Newcastle disease virus on virus shedding and transmission, *Viruses*, *9*, E225.

Liu, M., Zhao, X., Hua, S., Du, X., Peng, Y., Li, X., … Jiang, T. (2015). Antigenic patterns and evolution of the human influenza A (H1N1) virus. *Scientific Reports*, *5*, 14171.

Lundegaard, C., Lamberth, K., Harndahl, M., Buus, S., Lund, O., & Nielsen, M. (2008). NetMHC-3.0: Accurate web accessible predictions of human, mouse and monkey MHC class I affinities for peptides of length 8–11. *Nucleic Acids Research*, *36*, W509–512.

Luo, Y., Ji, S., Liu, Y., Lei, J. L., Xia, S. L., Wang, Y., … Qiu, H. J. (2017). Isolation and characterization of a moderately virulent classical swine fever virus emerging in China. *Transboundary and Emerging Diseases*, *64*, 1848–1857.

Meyers, G., & Thiel, H. J. (1996). Molecular characterization of pestiviruses. *Advances in Virus Research*, *47*, 53–118.

Moennig, V., Becher, P., & Beer, M. (2013). Classical swine fever. *Developments in Biologicals*, *135*, 167–174.

Moennig, V., Floegel-Niesmann, G., & Greiser-Wilke, I. (2003). Clinical signs and epidemiology of classical swine fever: A review of new knowledge. *Veterinary Journal*, *165*, 11–20.

Narula, A., Pandey, R. K., Khatoon, N., Mishra, A., & Prajapati, V. K. (2018). Excavating chikungunya genome to design B and T cell multi-epitope subunit vaccine using comprehensive immunoinformatics approach to control chikungunya infection. *Infection, Genetics and Evolution: Journal of Molecular Epidemiology and Evolutionary Genetics in Infectious Diseases*, *61*, 4–15.

Nielsen, M., Lundegaard, C., Worning, P., Lauemoller, S. L., Lamberth, K., Buus, S., … Lund, O. (2003). Reliable prediction of T-cell epitopes using neural networks with novel sequence representations. *Protein Science: A Publication of the Protein Society*, *12*, 1007–1017.

OIE, M. (2014). *Classical swine fever (Hog colera) in: OIE Manual of Diagnostic Tests and Vaccines* (pp. 1–25). Paris, France: Office International des Epizooties [chapter 2.8.3].

Peng, Y., Li, X., Zhou, H., Wu, A., Dong, L., Zhang, Y., … Jiang, T. (2017). Continual antigenic diversification in China leads to global antigenic complexity of avian influenza H5N1 viruses. *Scientific Reports*, *7*, 43566.

Perez, L. J., de Arce, H. D., Cortey, M., Dominguez, P., Percedo, M. I., Perera, C. L., … Nunez, J. I. (2011a). Phylogenetic networks to study the origin and evolution of porcine circovirus type 2 (PCV2) in Cuba. *Veterinary Microbiology*, *151*, 245–254.

Perez, L. J., de Arce, H. D., Tarradas, J., Rosell, R., Perera, C. L., Munoz, M., … Ganges, L. (2011b). Development and validation of a novel SYBR Green real-time RT-PCR assay for the detection of classical swine fever virus evaluated on different real-time PCR platforms. *Journal of Virological Methods*, *174*, 53–59.

Perez, L. J., Diaz de Arce, H., Barrera, M., Castell, S., & Frias, M. T. (2009). A polyclonal -antibody-immunoperoxidase-conjugate for the specific detection of porcine circovirus type 2. *Revista De Salud Animal*, *31*, 6.

Perez, L. J., Diaz de Arce, H., Perera, C. L., Rosell, R., Frias, M. T., Percedo, M. I., … Ganges, L. (2012a). Positive selection pressure on the B/C domains of the E2-gene of classical swine fever virus in endemic areas under C-strain vaccination. *Infection, Genetics and Evolution: Journal of Molecular Epidemiology and Evolutionary Genetics in Infectious Diseases*, *12*, 1405–1412.

Perez, L. J., Perera, C. L., Frias, M. T., Nunez, J. I., Ganges, L., & de Arce, H. D. (2012b). A multiple SYBR Green I-based real-time PCR system for the simultaneous detection of porcine circovirus type 2, porcine parvovirus, pseudorabies virus and Torque teno sus virus 1 and 2 in pigs. *Journal of Virological Methods*, *179*, 233–241.

Peters, B., Bulik, S., Tampe, R., Van Endert, P. M., & Holzhutter, H. G. (2003). Identifying MHC class I epitopes by predicting the TAP transport efficiency of epitope precursors. *Journal of Immunology*, *171*, 1741–1749.

Postel, A., Austermann-Busch, S., Petrov, A., Moennig, V., & Becher, P. (2018). Epidemiology, diagnosis and control of classical swine fever: Recent developments and future challenges. *Transboundary and Emerging Diseases*, *65*(Suppl 1), 248–261.

Postel, A., Pérez, L. J., Perera, C. L., Schmeiser, S., Meyer, D., Meindl-Boehmer, A., … Becher, P. (2015). Development of a new LAMP assay for the detection of CSFV strains from Cuba: A proof-of-concept study. *Archives of Virology*, *160*, 1435–1448.

Postel, A., Schmeiser, S., Perera, C. L., Rodriguez, L. J., Frias-Lepoureau, M. T., & Becher, P. (2013). Classical swine fever virus isolates from Cuba form a new subgenotype 1.4. *Veterinary Microbiology*, *161*, 334–338.

Pradhan, D., Yadav, M., Verma, R., Khan, N. S., Jena, L., & Jain, A. K. (2017). Discovery of T-cell driven subunit vaccines from Zika Virus genome: An immunoinformatics approach. *Interdisciplinary Sciences, Computational Life Sciences*, *9*, 468–477.

Reed, L. J., & Muench, H. (1938). A simple method of estimating fifty per cent endpoints. *American Journal of Epidemiology*, *27*, 493–497.

Ren, X., Li, Y., Liu, X., Shen, X., Gao, W., & Li, J. (2015). Computational identification of antigenicity-associated sites in the hemagglutinin protein of A/H1N1 seasonal influenza virus. *PLoS ONE*, *10*, e0126742.

Rios, L., Coronado, L., Naranjo-Feliciano, D., Martinez-Perez, O., Perera, C. L., Hernandez-Alvarez, L., … Perez, L. J. (2017). Deciphering the emergence, genetic diversity and evolution of classical swine fever virus. *Scientific Reports*, *7*, 17887.

Rios, L., Nunez, J. I., Diaz de Arce, H., Ganges, L., & Perez, L. J. (2018). Revisiting the genetic diversity of classical swine fever virus: A proposal for new genotyping and subgenotyping schemes of classification. *Transboundary and Emerging Diseases*, *65*, 963–971.

Schrodinger, L. L. C. (2015). The PyMOL molecular graphics system. *Version*, *1*, 8.

Shen, H., Pei, J., Bai, J., Zhao, M., Ju, C., Yi, L., … Chen, J. (2011). Genetic diversity and positive selection analysis of classical swine fever virus isolates in south China. *Virus Genes*, *43*, 234–242.

Silva, M. N., Silva, D. M., Leite, A. S., Gomes, A. L., Freitas, A. C., Pinheiro-Junior, J. W., … Jesus, A. L. (2017). Identification and genetic characterization of classical swine fever virus isolates in Brazil: A new subgenotype. *Archives of Virology*, *162*, 817–822.

Sorensen, M. R., Ilsoe, M., Strube, M. L., Bishop, R., Erbs, G., Hartmann, S. B., & Jungersen, G. (2017). Sequence-based genotyping of expressed swine leukocyte antigen class I alleles by next-generation sequencing reveal novel swine leukocyte antigen class I haplotypes and alleles in Belgian, Danish, and Kenyan Fattening Pigs and Gottingen Minipigs. *Frontiers in Immunology*, *8*, 701.

Soria-Guerra, R. E., Nieto-Gomez, R., Govea-Alonso, D. O., & Rosales-Mendoza, S. (2015). An overview of bioinformatics tools for epitope prediction: Implications on vaccine development. *Journal of Biomedical Informatics*, *53*, 405–414.

Stipp, S. R., Iniguez, A., Wan, F., & Wodarz, D. (2016). Timing of CD8 T cell effector responses in viral infections. *Royal Society Open Science*, *3*, 150661.

Stranzl, T., Larsen, M. V., Lundegaard, C., & Nielsen, M. (2010). NetCTLpan: Pan-specific MHC class I pathway epitope predictions. *Immunogenetics*, *62*, 357–368.

Tamura, T., Nagashima, N., Ruggli, N., Summerfield, A., Kida, H., & Sakoda, Y. (2014). Npro of classical swine fever virus contributes to pathogenicity in pigs by preventing type I interferon induction at local replication sites. *Veterinary Research*, *45*, 47.

Tamura, T., Sakoda, Y., Yoshino, F., Nomura, T., Yamamoto, N., Sato, Y., … Kida, H. (2012). Selection of classical swine fever virus with enhanced pathogenicity reveals synergistic virulence determinants in E2 and NS4B. *Journal of Virology*, *86*, 8602–8613.

Tang, F., Pan, Z., & Zhang, C. (2008). The selection pressure analysis of classical swine fever virus envelope protein genes Erns and E2. *Virus Research*, *131*, 132–135.

Tarradas, J., de la Torre, M. E., Rosell, R., Perez, L. J., Pujols, J., Munoz, M., … Ganges, L. (2014). The impact of CSFV on the immune response to control infection. *Virus Research*, *185*, 82–91.

Terpstra, C., Bloemraad, M., & Gielkens, A. L. J. (1984). The neutralizing peroxidase-linked assay for detection of antibody against swine fever virus. *Veterinary Microbiology*, *9*, 113–120.

Terpstra, C., & Wensvoort, G. (1988). The protective value of vaccine-induced neutralising antibody titres in swine fever. *Veterinary Microbiology*, *16*, 123–128.

Topfer, A., Hoper, D., Blome, S., Beer, M., Beerenwinkel, N., Ruggli, N., & Leifer, I. (2013). Sequencing approach to analyze the role of quasispecies for classical swine fever. *Virology*, *438*, 14–19.

Wang, J., Sun, Y., Meng, X. Y., Li, L. F., Li, Y., Luo, Y., … Qiu, H. J. (2018). Comprehensive evaluation of the host responses to infection with differentially virulent classical swine fever virus strains in pigs. *Virus Research*, *255*, 68–76.

Wang, Q., Wang, Z., Zhao, Y., Li, B., & Qiu, H. (2000). [Nucleotide sequence analysis of E2 major protective antigen encoding region of 12 strains of hog cholera virus(HCV)]. *Wei sheng wu xue bao = Acta Microbiologica Sinica*, *40*, 614–621.

Wang, X., Sun, Q., Ye, Z., Hua, Y., Shao, N., Du, Y., … Wan, C. (2016). Computational approach for predicting the conserved B-cell epitopes of hemagglutinin H7 subtype influenza virus. *Experimental and Therapeutic Medicine*, *12*, 2439–2446.

Ward, M. P. (2007). Spatio-temporal analysis of infectious disease outbreaks in veterinary medicine: Clusters, hotspots and foci. *Veterinaria Italiana*, *43*, 559–570.

Weesendorp, E., Stegeman, A., & Loeffen, W. (2009). Dynamics of virus excretion via different routes in pigs experimentally infected with classical swine fever virus strains of high, moderate or low virulence. *Veterinary Microbiology*, *133*, 9–22.

Wensvoort, G., Terpstra, C., Boonstra, J., Bloemraad, M., & Van Zaane, D. (1986). Production of monoclonal antibodies against swine fever virus and their use in laboratory diagnosis. *Veterinary Microbiology*, *12*, 101–108. https://doi.org/10.1016/0378-1135(86)90072-6

Xie, Z., Pang, D., Yuan, H., Jiao, H., Lu, C., Wang, K., … Ouyang, H. (2018). Genetically modified pigs are protected from classical swine fever virus. *PLoS Path*, *14*, e1007193. https://doi.org/10.1371/journal.ppat.1007193

Xing, C., Lu, Z., Jiang, J., Huang, L., Xu, J., He, D., … Gong, W. (2018). Sub-subgenotype 2.1c isolates of classical swine fever virus are dominant in Guangdong province of China, 2018. *Infection, Genetics and Evolution: Journal of Molecular Epidemiology and Evolutionary Genetics in Infectious Diseases*, *68*, 212–217. https://doi.org/10.1016/j.meegid.2018.12.029

Zhang, H., Leng, C., Tian, Z., Liu, C., Chen, J., Bai, Y., … Tong, G. (2018). Complete genomic characteristics and pathogenic analysis of the newly emerged classical swine fever virus in China. *BMC Veterinary Research*, *14*, 204. https://doi.org/10.1186/s12917-018-1504-2

SUPPORTING INFORMATION

Additional supporting information may be found online in the Supporting Information section at the end of the article.

How to cite this article: Coronado L, Rios L, Frías MT, et al. Positive selection pressure on E2 protein of classical swine fever virus drives variations in virulence, pathogenesis and antigenicity: Implication for epidemiological surveillance in endemic areas. *Transbound Emerg Dis*. 2019;66:2362–2382. https://doi.org/10.1111/tbed.13293